Mon. Not. R. Astron. Soc. **000**, 1–18 (2016) Printed 2 March 2016 (MN LATEX style file v2.2)

Constraining ultra-compact dwarf galaxy formation with galaxy clusters in the local universe

arXiv:1603.00032v1 [astro-ph.GA] 29 Feb 2016

J. Pfeffer[1,2⋆], M. Hilker[3], H. Baumgardt[1], B. F. Griffen[4]
[1] *School of Mathematics and Physics, The University of Queensland, Brisbane, QLD 4072, Australia*
[2] *Astrophysics Research Institute, Liverpool John Moores University, 146 Brownlow Hill, Liverpool L3 5RF, UK*
[3] *European Southern Observatory (ESO), Karl-Schwarzschild-Strasse 2, 85748 Garching, Germany*
[4] *Massachusetts Institute of Technology, Kavli Institute for Astrophysics and Space Research, 77 Massachusetts Avenue, Cambridge, MA 02139, USA*

ABSTRACT

We compare the predictions of a semi-analytic model for ultra-compact dwarf galaxy (UCD) formation by tidal stripping to the observed properties of globular clusters (GCs) and UCDs in the Fornax and Virgo clusters. For Fornax we find the predicted number of stripped nuclei agrees very well with the excess number of GCs+UCDs above the GC luminosity function. GCs+UCDs with masses $>10^{7.3}\,\mathrm{M}_\odot$ are consistent with being entirely formed by tidal stripping. Stripped nuclei can also account for Virgo UCDs with masses $>10^{7.3}\,\mathrm{M}_\odot$ where numbers are complete by mass. For both Fornax and Virgo, the predicted velocity dispersions and radial distributions of stripped nuclei are consistent with that of UCDs within ∼50-100 kpc but disagree at larger distances where dispersions are too high and radial distributions too extended. Stripped nuclei are predicted to have radially biased anisotropies at all radii, agreeing with Virgo UCDs at clustercentric distances larger than 50 kpc. However, ongoing disruption is not included in our model which would cause orbits to become tangentially biased at small radii. We find the predicted metallicities and central black hole masses of stripped nuclei agree well with the metallicities and implied black hole masses of UCDs for masses $>10^{6.5}\,\mathrm{M}_\odot$. The predicted black hole masses also agree well with that of M60-UCD1, the first UCD with a confirmed central black hole. These results suggest that observed GC+UCD populations are a combination of genuine GCs and stripped nuclei, with the contribution of stripped nuclei increasing toward the high-mass end.

Key words: methods: numerical – galaxies: dwarf – galaxies: formation – galaxies: interactions – galaxies: star clusters

1 INTRODUCTION

Ultra-compact dwarf galaxies (UCDs) are a new type of galaxy discovered just over 15 years ago in spectroscopic surveys of the Fornax galaxy cluster with sizes ($R_\mathrm{e} \lesssim 100$ pc) and luminosities ($-14 \lesssim M_V \lesssim -12$) intermediate between globular clusters (GCs) and dwarf galaxies (Hilker et al. 1999a; Drinkwater et al. 2000). Follow-up high resolution spectroscopy has found that UCDs have similar internal velocity dispersions to dwarf elliptical nuclei (σ ∼30 km s^{-1}, Drinkwater et al. 2003). Initially labelled UCDs (Phillipps et al. 2001) or dwarf-globular transition objects (Haşegan et al. 2005) their formation mechanism is still under debate, however two main scenarios have been suggested: they may be the high-mass end of the GC mass function observed around galaxies with rich GC systems (Mieske, Hilker & Infante 2002; Mieske, Hilker & Misgeld 2012) or the nuclei of tidally stripped dwarf galaxies (Bekki, Couch & Drinkwater 2001; Bekki et al. 2003; Drinkwater et al. 2003; Pfeffer & Baumgardt 2013).

Through dedicated surveys many new UCDs have been found (Mieske, Hilker, & Infante 2004a; Firth et al. 2007; Firth, Drinkwater, & Karick 2008; Gregg et al. 2009), to the point where the confirmed objects now number in the hundreds in the Fornax cluster alone (Mieske et al. 2012). UCDs have since been discovered in many environments, including other galaxy clusters (Abell 1689: Mieske et al. 2004b; Virgo: Haşegan et al. 2005; Jones et al. 2006; Centaurus: Mieske et al. 2007; Coma: Price et al. 2009; Chiboucas et al. 2010; Hydra I: Misgeld et al. 2011; Perseus: Penny et al. 2012), galaxy groups (Dorado and NGC 1400: Evstigneeva et al. 2007; NGC 5128: Rejkuba et al. 2007; HCG 22 and HCG 90: Da Rocha et al. 2011; NGC 3923: Norris & Kannappan 2011) and around isolated galaxies

⋆ E-mail: j.l.pfeffer@ljmu.ac.uk

© 2016 RAS

(NGC 7252: Maraston et al. 2004; Sombrero: Hau et al. 2009; NGC4546: Norris & Kannappan 2011). As more UCDs are found there is growing evidence that no single formation mechanism is responsible for their formation, however most UCDs either formed as giant GCs or by tidal stripping of nucleated dwarf galaxies (Haşegan et al. 2005; Mieske et al. 2006; Brodie et al. 2011; Chilingarian et al. 2011; Da Rocha et al. 2011; Norris & Kannappan 2011; Norris et al. 2014; Pfeffer et al. 2014). Although the formation mechanism of a few peculiar objects can be determined (e.g. Seth et al. 2014; Norris et al. 2015), disentangling the individual formation mechanism of most UCDs is almost impossible due to the similar predictions of internal UCD properties from each formation scenario. Determining the origin of UCDs therefore requires detailed predictions of how much each possible formation mechanism contributes to UCD populations.

Tidal stripping of nucleated galaxies is a likely origin for many UCDs (and a confirmed origin for two objects, Seth et al. 2014; Norris et al. 2015) however their contribution to the total UCD population is uncertain (and partly compounded by the various definitions of UCDs). Previous studies have shown that tidal stripping of nucleated galaxies can produce objects with similar properties to observed UCDs (Bekki et al. 2003; Pfeffer & Baumgardt 2013). A number of studies presented estimates for the number of UCDs formed due to tidal disruption (Bekki et al. 2003; Goerdt et al. 2008; Thomas, Drinkwater & Evstigneeva 2008). However as these estimates were based on UCD formation in clusters with static potentials they suffer from a number of problems. Static models do not take into account UCD formation that may have occurred within subclusters that later fell into the main cluster. Since galaxy clusters are expected to undergo many mergers during their formation, galaxies in clusters may be on chaotic orbits providing a few close pericentre passages necessary for UCD formation but far from the cluster centre at other times (Pfeffer & Baumgardt 2013)[1]. Galaxies orbiting in clusters may also have interactions with other satellite galaxies thereby making tidal disruption more likely.

In Pfeffer et al. (2014, hereafter P14) we presented the first model for UCD formation based on cosmological simulations of galaxy formation. Our model uses a semi-analytic galaxy formation model to select possible UCD progenitor galaxies and to determine when they become disrupted by tidal forces. Assuming that galaxies at high redshift have the same distribution of nucleus-to-galaxy mass and nucleation fraction as galaxies in the present day Universe we determined the numbers and masses of UCDs formed by tidal stripping. Some preliminary analysis was presented comparing the number of UCDs predicted with the observed number in the Fornax cluster, finding at most ∼10 per cent of UCDs have formed by tidal stripping.

In this paper we compare in detail the predictions of the P14 model with the properties of UCDs from the Fornax and Virgo clusters. In particular we compare the predicted mass functions, radial and velocity distributions, metallicities and central black hole masses with the observed distributions. Throughout the paper we refer to objects formed in the simulation by tidal stripping of nucleated galaxies as stripped nuclei since such objects may resemble both GCs and UCDs and because the observed UCD populations may be the result of more than one formation channel.

This paper is organized as follows. Section 2 describes the criteria for selecting analogue galaxy clusters of the Fornax and Virgo clusters and briefly summarises the method of P14 for identifying stripped nuclei in cosmological simulations. Section 3 describes the compilation of observational data of GCs, UCDs and dwarf galaxies. Section 4 presents the results comparing the simulation and observational data. In Section 5 and 6 we discuss the implications of our work for UCD formation scenarios and summarize our results.

2 SEMI-ANALYTIC MODELLING

Here we summarize the stripped nucleus formation model of P14 and detail our selection criteria for comparing against observed galaxy clusters.

The model makes use of the semi-analytic galaxy formation model (SAM) of Guo et al. (2011, hereafter G11) which was applied to the subhalo merger trees of the Millennium-II simulation (Boylan-Kolchin et al. 2009, hereafter MS-II). The MS-II is a cosmological dark-matter only simulation which has a box size of 137 Mpc and a particle mass of $9.42 \times 10^6\,\mathrm{M}_\odot$. The G11 SAM is constrained by low-redshift galaxy abundance and clustering in the Sloan Digital Sky Survey and is tuned to reproduce the $z = 0$ mass distribution of galaxies down to stellar masses of $10^{7.5}\,\mathrm{M}_\odot$. In the G11 SAM satellite galaxies (i.e. those currently or previously at the centre of non-dominant haloes orbiting within a more massive halo) may have either resolved or unresolved dark matter (DM) haloes under the assumption that the stellar component of a satellite galaxy is harder to disrupt than its halo. For the stellar component of a satellite galaxy to be disrupted its DM halo must first be entirely dissolved (i.e. become unresolved). Since tidal stripping is not taken into account in the model, satellite galaxies do not lose stellar mass until they are completely disrupted. For all data associated with MS-II and the G11 SAM we assume a cosmology consistent with the *Wilkinson Microwave Anisotropy Probe* 1-year data (WMAP1) results (Spergel et al. 2003) and assume $h = 0.73$ for all masses and distances[2]. The data associated with the MS-II and G11 SAM are publicly provided by the Virgo-Millennium Database (Lemson & Virgo Consortium 2006)[3].

In P14 a sample of galaxy clusters was chosen such that $M_{\rm vir} > 10^{13}\,\mathrm{M}_\odot/h$. Here we limit the cluster sample according to the mass of the cluster we are comparing with. For the Fornax cluster we choose all clusters within the range $M_{\rm vir} = 7 \pm 2 \times 10^{13}\,\mathrm{M}_\odot$ (Drinkwater et al. 2001),

[1] However this study neglected dark matter in the dwarf galaxies and used unrealistic orbits and therefore may overestimate the ability of tidal stripping to form UCDs.

[2] In P14 we tested semi-analytic models for both a WMAP1 (Guo et al. 2011) and WMAP7 cosmology (Guo et al. 2013), finding no significant difference between the predictions. Therefore modelling with an updated cosmology would not change our results.

[3] `http://www.mpa-garching.mpg.de/millennium`

giving 37 clusters for comparison. For the Virgo cluster we choose all clusters within the range $M_{\rm vir} = (1.4–7)\times10^{14}$ M$_\odot$ (McLaughlin 1999; Tonry et al. 2000; Urban et al. 2011), giving 13 clusters for comparison.

After the SAM clusters are chosen, stripped nuclei are identified in the simulations in the following way:

(i) The galaxy merger trees of all galaxies in the SAM clusters at $z = 0$ are searched for possible stripped nucleus progenitors (hereafter referred to as candidate galaxies and the DM halo of the galaxies as candidate haloes). A galaxy is defined as a possible progenitor when the stellar mass exceeds $10^{7.5}$ M$_\odot$ (i.e. all progenitors of the candidate galaxy have a stellar mass less than this limit). This lower mass cut is chosen based on the lower mass limit observed for nucleated galaxies (see figure 1 of P14).

(ii) To form a stripped nucleus the candidate galaxy must undergo a merger with a more massive galaxy and the stellar component of the galaxy be completely disrupted according to the criteria in the SAM (equation 30 of G11). It is assumed that during this process the nuclear cluster of the galaxy is not disrupted since it is much more compact than the galaxy (Bekki et al. 2003; Pfeffer & Baumgardt 2013).

(iii) The galaxy merger must be a minor merger[4], where a minor merger is defined as those with 'dynamical' mass ratios smaller than 1:3. The dynamical mass $M_{\rm dyn}$ is defined as $M_{\rm dyn} = M_* + M_{\rm gas} + M_{\rm DM}(< r_{\rm s})$ where M_* is the stellar mass of the galaxy, $M_{\rm gas}$ is the cold gas mass and $M_{\rm DM}(< r_{\rm s})$ is the mass of the DM halo within the NFW scale radius.

(iv) The candidate galaxy merged[5] (i.e. the stellar component of the galaxy was disrupted according to the SAM) at least 2 Gyr ago so there is enough time to form a UCD (Pfeffer & Baumgardt 2013).

(v) The dynamical friction time of the stripped nucleus $t_{\rm friction}$ (determined using equation 7-26 from Binney & Tremaine 1987) is calculated at the snapshot before the candidate galaxy is disrupted. After a time $t_{\rm friction}$ the stripped nucleus is assumed to merge with the centre of the galaxy it is orbiting and therefore be completely disrupted. This differs from the treatment of dynamical friction in P14 where the dynamical friction time was calculated for the halo the stripped nucleus is associated with at $z = 0$. We find the predictions of the model are unaffected by this change.

After the candidate galaxy is disrupted the stripped nucleus takes the position and velocity of the most bound particle of the candidate halo (similar to galaxies without resolved haloes in the G11 SAM). We also take into account orbital decay of the stripped nuclei due to dynamical friction by modifying the distance of the stripped nuclei from their host galaxies by a factor $(1 - \Delta t/t_{\rm friction})$, where Δt is the time since the progenitor galaxy was disrupted (this is identical to the treatment of satellite galaxies in the G11 SAM). The velocity of the stripped nucleus relative to the host galaxy was kept the same as the velocity of the most bound particle relative to the host halo (to account for galaxies undergoing orbital decay in the SAM).

The two main assumptions for assigning physical properties to the stripped nuclei are the following:

(i) The stripped nucleus is assigned a mass randomly chosen from a log-normal mass function for the nucleus-to-galaxy mass ratio $M_{\rm nuc}/M_{*,\rm gal}$ (where the mass of the candidate galaxy is taken immediately before disruption). Based on figure 14 from Côté et al. (2006), we choose a mean of 0.3 per cent and a log-normal standard deviation of 0.5 dex. Tidal stripping of the stripped nuclei is not taken into account. Recently, Georgiev et al. (2016) found $M_{\rm nuc}/M_{*,\rm gal} \simeq 0.1$ per cent in both early- and late-type galaxies, lower than the value we assumed. Therefore when comparing mass functions in Section 4.1 we also consider this value for the nucleus-to-galaxy mass ratio.

(ii) The fraction of galaxies that are nucleated is taken from observations of galaxies in the Virgo and Fornax clusters (see figure 1 of P14). For galaxies between stellar masses of 3.0×10^7 and 4.7×10^8 M$_\odot$ we choose a nucleation fraction that varies linearly (in log-space) between 0 and 80 per cent. Between stellar masses of 4.7×10^8 and 10^{11} M$_\odot$ we take an average nucleation fraction of 80 per cent. For galaxies above stellar masses of 10^{11} M$_\odot$ we assume nuclear clusters are destroyed by supermassive black holes (e.g. Graham & Spitler 2009). Where possible, to improve our statistics we work with fractions of stripped nuclei instead of randomly choosing galaxies to satisfy the nucleated fraction.

3 OBSERVATIONAL DATA

For all data associated with the Fornax cluster we use the distance modulus $m - M = 31.39$ mag (Freedman et al. 2001) corresponding to a distance of 19 Mpc and a spatial scale of 92 pc arcsec^{-1}. For all data associated with the Virgo cluster we use the distance modulus $m - M = 31.09$ mag (Mei et al. 2007) corresponding to a distance of 16.5 Mpc and a spatial scale of 80 pc arcsec^{-1}.

3.1 Fornax cluster

3.1.1 GCs and UCDs

Since UCDs were discovered, the GC and UCD population of the Fornax cluster has been the subject of many studies. To determine the number of spectroscopically confirmed GCs+UCDs in Fornax we compile the number and luminosities of objects from Hilker et al. (1999a), Drinkwater et al. (2000), Mieske et al. (2002, 2004a), Bergond et al. (2007), Hilker et al. (2007), Firth et al. (2007), Mieske et al. (2008), Gregg et al. (2009), Schuberth et al. (2010), Chilingarian et al. (2011) and Puzia & Hilker (priv. comm.). The total number of confirmed GCs+UCDs in the Fornax cluster is 935. Due to the 2dF Fornax surveys of Drinkwater et al. (2000) and Gregg et al. (2009), the number of GCs+UCDs with luminosities brighter than $M_V < -11.5$ mag are more than 95 per cent complete within a clustercentric radius of 0.9 degrees, or

[4] It is important to note that in the minor merger process we expect the candidate galaxy was disrupted by the tidal field of the host galaxy. In this case the nuclear cluster of the galaxy is not disrupted and forms a UCD (Bekki et al. 2003; Pfeffer & Baumgardt 2013). In the case of a major merger the nuclei of the two galaxies merge and a UCD is not produced.

[5] Galaxy mergers in the model are assumed to happen on a time scale shorter than the time between simulation snapshots (a maximum of 377 Myr) which may not be true in reality.

∼300 kpc. As most studies concentrated on the inner 15 acrmin of the cluster, or <83 kpc, the number of GCs+UCDs with luminosities $M_V < -10.25$ is approximately complete within 50 kpc and the completeness drops to below 70 per cent beyond this radius (see discussion in Mieske et al. 2012).

To compare the model predictions with the observed population it is necessary to derive masses for the GCs and UCDs from population synthesis models. GCs are generally very old (∼ 13 Gyr, Marín-Franch et al. 2009) and are consistent with having a Kroupa/Chabrier stellar initial mass function (IMF; e.g. McLaughlin & van der Marel 2005; Paust et al. 2010). Note that GCs actually show a spread in MFs due to ongoing dissolution, however at the high mass end for GCs which we are interested in this is not important (Baumgardt & Makino 2003). UCDs on the other hand are on average slightly younger than GCs (∼ 11 Gyr, Francis et al. 2012). Many UCDs have dynamical mass-to-light (M/L) ratios above what can be explained by stellar population models (Haşegan et al. 2005; Dabringhausen et al. 2008; Mieske et al. 2013). One suggestion is that the elevated M/L ratios are due to a top-heavy IMF (Dabringhausen, Kroupa, & Baumgardt 2009; Dabringhausen et al. 2012, although see also Phillipps et al. 2013). Therefore an IMF leading to higher masses should also be considered. To determine the effect of the assumed stellar population on our results we consider a number of different IMFs and simple stellar population (SSP) models. We use the Maraston (2005, M05) SSP model with Kroupa (2001) and Salpeter (1955) IMFs and the Bruzual & Charlot (2003, BC03) SSP model with a Chabrier (2003) IMF. Each SSP model is generated for two different ages, 11 and 13 Gyr. For the M05 models we tested both blue (bHB) and red horizontal branch (rHB) models but find no difference between the results and therefore only consider the rHB models hereafter. Masses for the GCs+UCDs were then calculated from the $(V-I)$-M/L_V relation fitted to the different SSP models (see also Misgeld & Hilker 2011). Given the observed properties of GCs and UCDs the Kroupa/Chabrier SSP models are the most reasonable. The Salpeter IMF (which is a bottom-heavy IMF compared to Kroupa/Chabrier) represents the case of elevated M/L ratios. In terms of mass, the completeness of $M_V < -11.5$ mag within 300 kpc corresponds to $M \gtrsim 10^{6.9}\,\mathrm{M}_\odot$ for the Kroupa/Chabrier SSP models.

To estimate the completeness of the Fornax sample within 83 kpc in terms of mass we compare the number of spectroscopically confirmed GCs+UCDs with the GC luminosity function (GCLF, derived from photometry, where the errors come from uncertainties in background corrections) within 83 kpc ($6,450 \pm 700$ GCs, Dirsch et al. 2003) and 300 kpc ($11,100 \pm 2,400$ GCs, Gregg et al. 2009, derived from the data of Bassino et al. 2006). It is assumed that the GCLF has a Gaussian shape with a width $\sigma = 1.3$ mag and peak $M_V = -7.6$ mag (Dirsch et al. 2003). We convert the GCLF to a mass function for a given SSP model/IMF assuming a constant M/L ratio given by median of the GC+UCD sample (to be dominated by objects with masses $\sim 10^6\,\mathrm{M}_\odot$) using 13 Gyr ages. In Fig. 1 we compare the number of spectroscopically confirmed GCs+UCDs with the GCLF for each SSP model. Comparing the results of all SSP models for the GC+UCD sample with the GCLF we estimate a completeness limit of $\sim 10^{6.7}\,\mathrm{M}_\odot$ within 83 kpc.

3.1.2 Dwarf galaxies

We take the sample of Fornax dwarf galaxies from the Fornax Cluster Catalogue (FCC, Ferguson 1989) with updated radial velocities from Thomas et al. (2008). We exclude one galaxy (FCC2) as a background galaxy due to its high line-of-sight velocity ($cz = 4540$ km s^{-1}) compared to the cluster ($cz \sim 1500$ km s^{-1}, Gregg et al. 2009). The catalogue is complete to $B_\mathrm{T} \sim 18$ mag, or $M_B \sim -13.4$ mag, and therefore we take this as the lower luminosity limit for the sample. Assuming a stellar mass-to-light ratio $M/L_B = 3\,(\mathrm{M/L})_\odot$ (typical for dwarf ellipticals, Chilingarian 2009) this corresponds to a stellar mass $M_* = 10^8\,\mathrm{M}_\odot$. A galaxy is considered to be a dwarf galaxy if it has a luminosity $M_B > -19.6$, corresponding to $M < 10^{10.5}\,\mathrm{M}_\odot$ for $M/L_B = 3\,(\mathrm{M/L})_\odot$. Therefore when comparing against dwarf galaxies in the FCC, we choose dwarf galaxies in the simulations that have stellar masses $10^8 < M_*/\,\mathrm{M}_\odot < 10^{10.5}$.

3.2 Virgo cluster

3.2.1 GCs and UCDs

The recent Next Generation Virgo cluster Survey (NGVS, Ferrarese et al. 2012), together with spectroscopic follow-up (Zhang et al. 2015), allows for a systematic comparison with UCDs in the Virgo cluster. Virgo cluster UCDs, specifically UCDs around the central galaxy M87, were therefore taken from Zhang et al. (2015). Objects selected from the NGVS have luminosities $M_g \leqslant -9.6$ mag and effective radii $R_e \geqslant 11$ pc, while previously confirmed objects selected from HST imaging (Brodie et al. 2011) have effective radii $R_e > 9.5$ pc. All UCDs selected have an upper size limit $R_e \lesssim 100$ pc. The total number of UCDs in the Zhang et al. (2015) catalogue is 97. The number of UCDs is expected to be nearly 100 per cent complete within 288 kpc for $g < 20.5$ mag. However, in the Zhang et al. (2015) study UCDs are defined by effective radius ($10 \lesssim R_e/\mathrm{pc} \lesssim 100$) while in our model we can currently only compare objects by mass. With this shortcoming in mind, in this work we give basic comparisons between Virgo UCDs and our model. More detailed analysis therefore requires observations that are complete above a given mass or a model which can predict stripped nuclei sizes.

To derive masses for the Zhang et al. (2015) sample of UCDs we follow the method of Misgeld & Hilker (2011). The apparent g_AB-band magnitudes were transformed into absolute V-band magnitudes using the relation $V = g_\mathrm{AB} + 0.026 - 0.307 \times (g z)_\mathrm{AB}$ given in Peng et al. (2006) and a Virgo distance modulus of 31.09 mag (Mei et al. 2007). Mass-to-light ratios M/L_V were calculated assuming a M/L_V-$(g-z)_\mathrm{AB}$ relation according to Maraston (2005) single stellar population models (Kroupa IMF, red horizontal branch) for ages of 11 and 13 Gyr (Misgeld & Hilker 2011). For objects H30772 and S887 we take z-band magnitudes from Jordán et al. (2009). For the luminosity completeness limit $g < 20.5$ mag, this corresponds to a completeness in mass of $M \gtrsim 10^{6.6}\,\mathrm{M}_\odot$.

To compare velocity dispersions of stripped nuclei with

GCs we use the sample of GCs compiled by Strader et al. (2011, excluding any UCDs defined in Zhang et al. 2015). For comparing radial number profiles of GCs around M87 we use the Sérsic profiles fitted by Zhang et al. (2015) to the surface number density profiles for blue [$0.55 < (g' - i')_0 < 0.80$] and red [$0.80 < (g' - i')_0 < 1.15$] GCs ($20 < g'_0 < 24$) determined by Durrell et al. (2014) using NGVS photometry. The profiles for the blue and red GCs were fitted within 240 and 120 kpc from M87, respectively.

3.2.2 Dwarf galaxies

For comparing the radial distribution of Virgo cluster galaxies we take the sample of dwarf galaxies from the Virgo Cluster Catalogue (VCC, Binggeli et al. 1985, excluding galaxies classified as background galaxies). The catalogue is complete to $B_{\rm T} \sim 18$ mag, or $M_B \sim -13.1$ mag. As for the Fornax cluster, we assume a typical mass-to-light ratio of $M/L_B = 3\,({\rm M/L})_\odot$ and use a stellar mass cut when comparing with simulations of $10^8 < M_*/\,{\rm M}_\odot < 10^{10.5}$.

For comparing velocities of Virgo cluster galaxies we take the sample of dwarf galaxies from the Extended Virgo Cluster Catalogue (EVCC, Kim et al. 2014). Masses for the dwarf galaxies were again estimated following the method of Misgeld & Hilker (2011). The apparent $g_{\rm AB}$-band magnitudes were transformed into absolute V-band magnitudes using the relation given in Peng et al. (2006). Mass-to-light ratios M/L_V were calculated assuming a M/L_V-$(g-z)_{\rm AB}$ relation according to Maraston (2005) single stellar population models (Kroupa IMF, blue horizontal branch) for ages of 11 Gyr. For comparison with the simulations we use a mass cut of $10^8 < M_*/\,{\rm M}_\odot < 10^{10.5}$.

3.3 GC and UCD metallicities

We compile a list of GC and UCD metallicities for Fornax and Virgo cluster GCs and UCDs from Mieske et al. (2008), Chilingarian et al. (2011) and Francis et al. (2012). Where possible we use the dynamical masses measured for objects in this sample. For common objects between the Mieske et al. (2008) and Chilingarian et al. (2011) samples we take data from Chilingarian et al.. For common objects between the Mieske et al. (2008) and Francis et al. (2012) samples we take data from Francis et al.. For the Chilingarian et al. sample we use the dynamical mass-to-light ratios to calculate the UCD masses where possible. For the Francis et al. sample we take dynamical masses from Mieske et al. (2013) for objects UCD1, UCD5, VUCD3 and VUCD5. For the other objects masses were calculated using the g and r colours and the stellar mass-to-light relations of Bell et al. (2003). For NGC1407-GC1 the g and r colours were taken from Romanowsky et al. (2009). For NGC1407 we assume a distance modulus of 31.99 mag (Jerjen, Tully, & Trentham 2004).

4 RESULTS

4.1 Mass function

In Fig. 1 we compare the cumulative mass function of simulated stripped nuclei in Fornax-like clusters with the number of confirmed Fornax GCs+UCDs compiled in Section 3.1 and the GCLF within 83 kpc (Dirsch et al. 2003) and 300 kpc (Gregg et al. 2009, derived from the data of Bassino et al. 2006) for each SSP model. The luminosity functions were converted to mass functions using a mass-to-light ratio given by the median of the Fornax GC+UCD sample for a given SSP model/IMF with an age of 13 Gyr. The luminosity function is approximated as a Gaussian with a width $\sigma = 1.3$ mag and peak magnitude of $M_V = -7.6$ mag (Dirsch et al. 2003) with a total of $6,450 \pm 700$ GCs within 83 kpc (Dirsch et al. 2003) and $11,100 \pm 2,400$ GCs within 300 kpc (Gregg et al. 2009). The figure suggests an excess of ~ 10 GCs+UCDs with masses $\gtrsim 10^7\,{\rm M}_\odot$ compared to the GC mass function. As noted by Gregg et al. (2009), given the low number of objects at the high mass/luminosity end, the number of UCDs is consistent with being the high-mass tail of the GC mass function. The most massive Fornax UCD (UCD3) is also very extended ($R_{\rm eff} = 90$ pc, Hilker et al. 2007) while all other Fornax UCDs have sizes less than 30 pc (e.g. Misgeld & Hilker 2011). This may indicate UCD3 is not part of the GC mass function even if its mass is consistent with being part of it (although GCs+UCDs formed by hierarchical merging of star clusters in cluster complexes may also reach such sizes, Brüns & Kroupa 2012). However, unlike M60-UCD1 (the most massive UCD in the Virgo cluster) which has a supermassive black hole (SMBH) containing 15 per cent of its mass and which was most likely formed by tidal stripping (Seth et al. 2014), UCD3 does not seem to have a SMBH (at least not one containing more than 5 per cent of its mass, Frank et al. 2011).

As already noted in P14, for masses more than $10^6\,{\rm M}_\odot$ the number of stripped nuclei predicted by the model is a factor > 20 smaller than the number of observed GCs+UCDs (~ 500, while the number inferred from the GCLF is ~ 1000). For masses between 10^6 and $10^7\,{\rm M}_\odot$ and $M_{\rm nuc}/M_{*,\rm gal} = 0.3$ per cent we predict that stripped nuclei account for ~ 2.5 per cent of GCs+UCDs. For masses larger than $10^7\,{\rm M}_\odot$ we predict stripped nuclei account for ~ 40 per cent of GCs+UCDs and become the dominant formation mechanism for masses larger than $\sim 10^{7.1}\,{\rm M}_\odot$ for a Kroupa/Chabrier IMF. When assuming $M_{\rm nuc}/M_{*,\rm gal} = 0.1$ per cent the predicted number of stripped nuclei decreases by a factor $\sim$2. As the number of dwarf galaxies at the centre of galaxy clusters is over-predicted by 50 per cent in the G11 SAM (Weinmann et al. 2011, see also Fig. 7), the number of predicted stripped nuclei might increase by a factor of two if more efficient tidal processes were implemented in the simulations[6]. However this is still too low to account for all observed UCDs.

In Fig. 2 we show the cumulative mass function for simulated stripped nuclei in Fornax-sized galaxy clusters compared with the difference of the number of spectroscopically confirmed GCs+UCDs with the GCLF for each SSP model: i.e. the excess number of objects which cannot be accounted

[6] Although the over-abundance of dwarf galaxies might also be related to the too efficient star formation in low-mass galaxies at early times or the over-clustering of galaxies at scales below 1 Mpc (Guo et al. 2011). See section 5.2 in P14 for a discussion about how this affects our predictions.

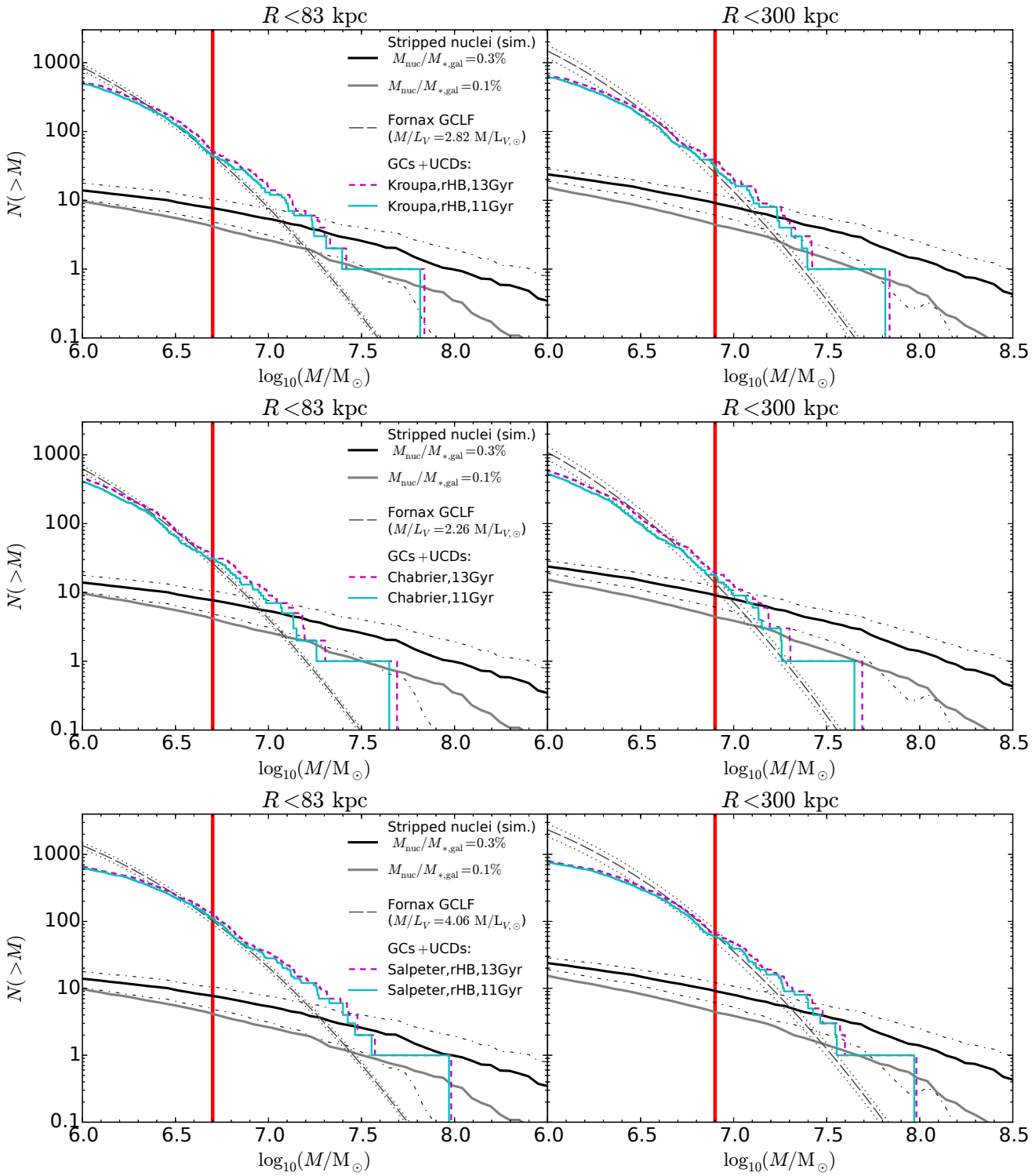

Figure 1. Cumulative mass function of simulated stripped nuclei in Fornax-like clusters assuming $M_{\rm nuc}/M_{*,\rm gal}$ is 0.3 per cent (black line, with standard deviation between clusters shown by black dash-dotted lines) and 0.1 per cent (grey line) compared with the number of spectroscopically confirmed Fornax GCs+UCDs (solid line, from Section 3.1) and the cumulative Fornax GC luminosity function (GCLF, long-dashed line with the error shown by dotted lines) within 83 kpc ($6,450 \pm 700$ GCs, Dirsch et al. 2003) and 300 kpc of NGC 1399 ($11,100 \pm 2,400$ GCs, Gregg et al. 2009, derived from the data of Bassino et al. 2006). The top panel shows the results for the Maraston (2005) SSP model with a Kroupa IMF, the middle panel for the Bruzual & Charlot (2003) SSP model with a Chabrier IMF and the bottom panel for the Maraston (2005) SSP model with a Salpeter IMF. In each panel we show the results for the Fornax GC+UCD sample with SSP ages of 13 (dashed magenta lines) and 11 Gyr (solid cyan lines). The luminosity functions were converted to mass functions in each panel using the median M/L ratio for the 13 Gyr SSP model (the M/L ratio is given in the legend of each panel). The vertical red lines show the estimated completeness of the confirmed GCs+UCDs.

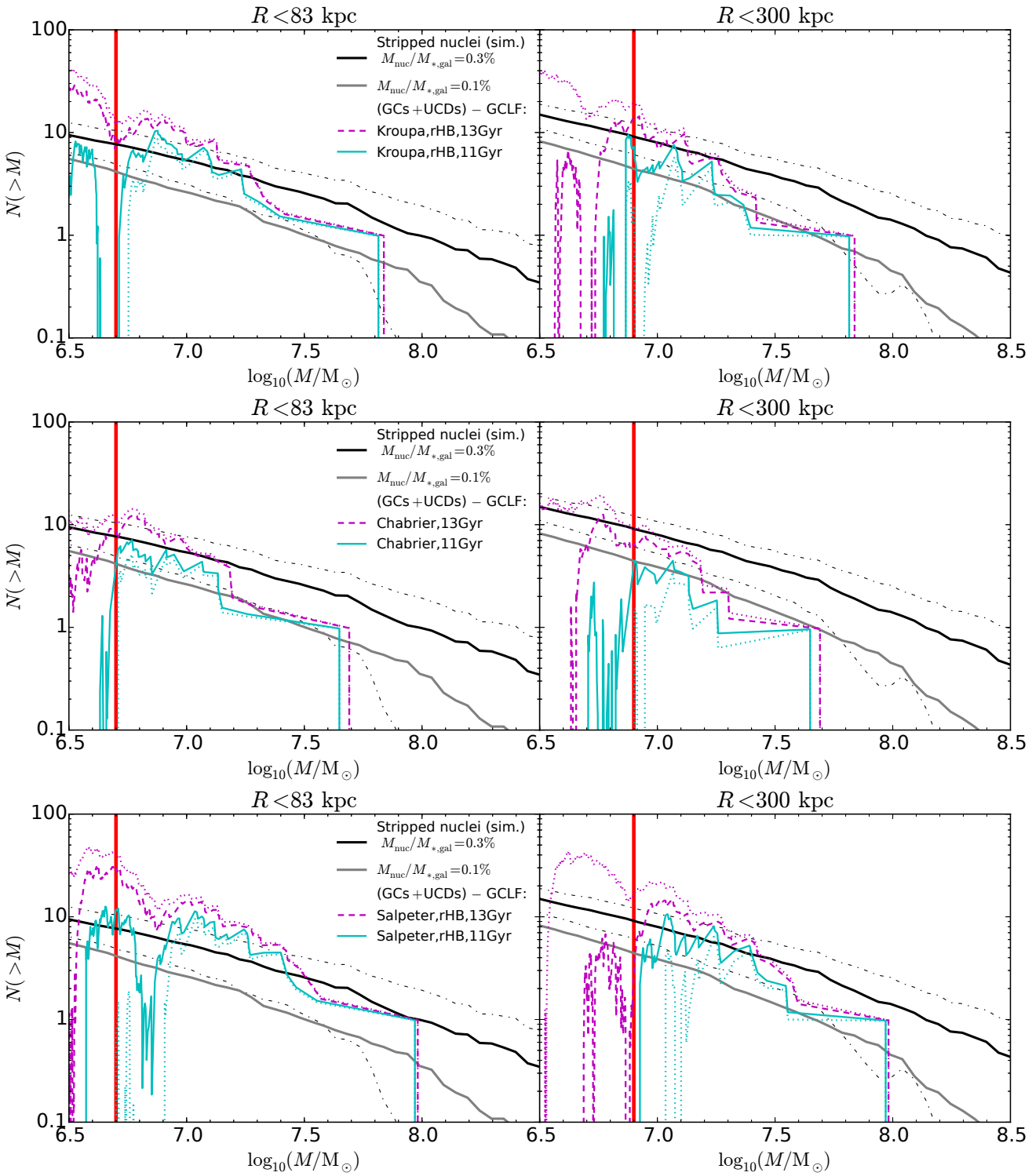

Figure 2. Cumulative mass function of simulated stripped nuclei in Fornax-like clusters within a projected distance of 83 (left panel) and 300 kpc (right panel) from the central galaxy assuming $M_{\rm nuc}/M_{*,\rm gal}$ is 0.3 per cent (black line, with standard deviation between clusters shown by black dash-dotted lines) and 0.1 per cent (grey line) compared with the difference of the Fornax GC+UCD sample and the GCLF [(GCs+UCDs)−GCLF] from Fig. 1. In each panel the results for SSP ages of 13 and 11 Gyr are shown by dashed magenta lines and solid cyan lines, respectively. The dotted lines show the upper limit for the 13 Gyr SSP (magenta) and lower limit for the 11 Gyr SSP (cyan) due to the error in the GCLF (the lower limit for the 13 Gyr SSP and upper limit for the 11 Gyr SSP are omitted for clarity). Vertical red lines show the estimated completeness of the confirmed GCs+UCDs.

for by the GCLF. The number of excess GCs+UCDs above the GCLF is slightly higher within 83 kpc than within 300 kpc which may indicate the number of objects beyond 83 kpc is not complete. Overall, given the uncertainties in our model, the SSP models and the GCLF, the agreement between our model and the excess number of GCs+UCDs in the Fornax cluster is very good. Within 83 kpc the predicted number of stripped nuclei agree well with the excess number of GCs+UCDs for all SSP models. Within 300 kpc the predicted number of stripped nuclei agree well with the number of GCs+UCDs above the GCLF for the Salpeter IMF. For the Kroupa and Chabrier IMFs the number of stripped nuclei predicted is too large above masses of $\sim 10^{7.3}$ M$_\odot$. Above masses of $\sim 10^{8}$ M$_\odot$ the number of stripped nuclei predicted may be too large, although the scatter in the simulations is large at the high-mass end given the small number of objects and stochastic nature of galaxy mergers.

The good agreement between the predicted number of stripped nuclei and the excess of GCs+UCDs above the GCLF implies that the observed number of GCs+UCDs can be described by a combination of the GCLF and stripped nuclear clusters. This suggests the most massive 'genuine GC'[7] has a mass of $\sim 10^{7.3}$ M$_\odot$. This is in good agreement with the most massive GC suggested from the NGC1399 GC luminosity function (Hilker 2009) and that suggested using a physically-motivated Toomre argument (which is found to describe very well the mass of young massive cluster populations, Adamo et al. 2015): Based on the most massive giant molecular clouds observed at high-redshift (Toomre mass $\sim 10^{9}$ M$_\odot$ at $z > 2$, Genzel et al. 2011), Kruijssen (2014) derived a maximum GC mass at formation of $10^{7.5}$ M$_\odot$ in high-redshift environments (in particular for possible progenitors of massive galaxies like NGC1399). After taking into account mass-loss due to stellar evolution such an object would have a present day mass of $\sim 10^{7.3}$ M$_\odot$, remarkably consistent with the most massive genuine GC suggested from our analysis.

Given the low numbers involved, distinguishing between a scenario where all UCDs are genuine GCs or one where UCDs are a combination of stripped nuclei and genuine GCs is nearly impossible by numbers alone. However, a combination of the Fornax GC luminosity function and the predicted mass function for stripped nuclei shows good agreement with the observed mass function of GCs+UCDs in the Fornax cluster. For masses larger than the completeness limits there is some evidence the GC+UCD mass function is better fit by a combination of the GCLF and stripped nucleus mass function (6.4 and 4.9 per cent agreement within 83 and 300 kpc, respectively, according to a KS test, averaged over all SSP models) than the GCLF alone (1.6 and 1.7 per cent agreement within 83 and 300 kpc, respectively, according to a KS test, averaged over all SSP models).

In Fig. 3 we show the cumulative mass functions of Virgo cluster UCDs and simulated stripped nuclei in Virgo-sized galaxy clusters within 288 kpc of the central galaxy (M87 for the Virgo cluster). It must be kept in mind that here UCDs are defined as having sizes $R_e \gtrsim 10$ pc while for the stripped nuclei a size cut is not possible with our model.

[7] I.e. formed through the same process as the majority of GCs and not as the nuclear star cluster of a galaxy.

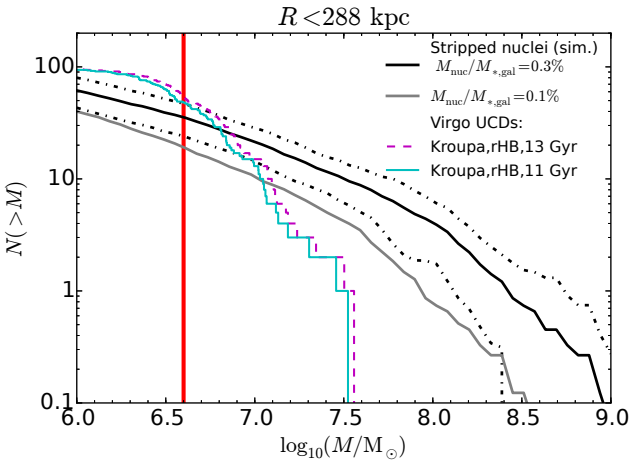

Figure 3. Cumulative mass function of simulated stripped nuclei in Virgo-sized galaxy clusters within a projected distance of 288 kpc from the central galaxy (dashed line with the standard deviation between clusters shown by dash-dotted lines) compared with UCDs ($R_e \gtrsim 10$ pc) in the Virgo cluster (thick solid line). The dashed magenta and solid cyan lines show UCDs masses using the Maraston (2005) SSP model with a Kroupa IMF for ages of 13 and 11 Gyr, respectively. The vertical red line shows the estimated completeness of the UCDs.

Above masses of $\sim 10^{7.3}$ M$_\odot$ all observed GCs and UCDs have sizes larger than ~ 10 pc (e.g. Misgeld & Hilker 2011; Norris et al. 2014) and therefore reasonable comparisons can be made above this mass. For Virgo-sized clusters there are significantly more high-mass ($M > 10^{7.5}$ M$_\odot$) stripped nuclei predicted than the observed number of UCDs (although in absolute terms it is only a difference of 4-5 objects). Above masses of $\sim 10^{6.6}$ M$_\odot$ the total predicted number of stripped nuclei is close to the number of observed UCDs and therefore in principle stripped nuclei can account for all observed objects. However at lower masses there are more observed objects than predicted by a factor ~ 2, with the difference likely being even larger given the incompleteness. The slope of the mass function predicted for stripped nuclei also differs from that of the UCDs: Over the mass range $10^{6.6}$-$10^{7.9}$ M$_\odot$ stripped nuclei have a power law slope $\alpha_{\rm SN} = -0.62$ while Virgo UCDs have a slope $\alpha_{\rm UCDs} = -1.4$. This may be an indication that the galaxy disruption criterion is too efficient for high-mass galaxies, our assumption of a constant nucleus-to-galaxy mass ratio $M_{\rm nuc}/M_{*,\rm gal}$ with redshift is inaccurate, $M_{\rm nuc}/M_{*,\rm gal}$ of the most massive nucleated galaxies is decreased (some hints of this is shown for galaxies with $M_{*,\rm gal} \sim 10^{11}$ M$_\odot$ in fig. 6(c) of Georgiev et al. 2016) or the nucleation fraction of galaxies with $M_{*,\rm gal} \sim 10^{11}$ M$_\odot$ is less than the 80 per cent we assumed. As we do not predict sizes for the stripped nuclei it is also possible that the most massive objects would have sizes too large to be considered UCDs (i.e. $R_e > 100$ pc) and therefore should not be included in the comparison.

4.2 Kinematics

In this section we compare the kinematic predictions for our model stripped nuclei and dwarf galaxies from the G11 SAM with observations in the Fornax and Virgo clusters.

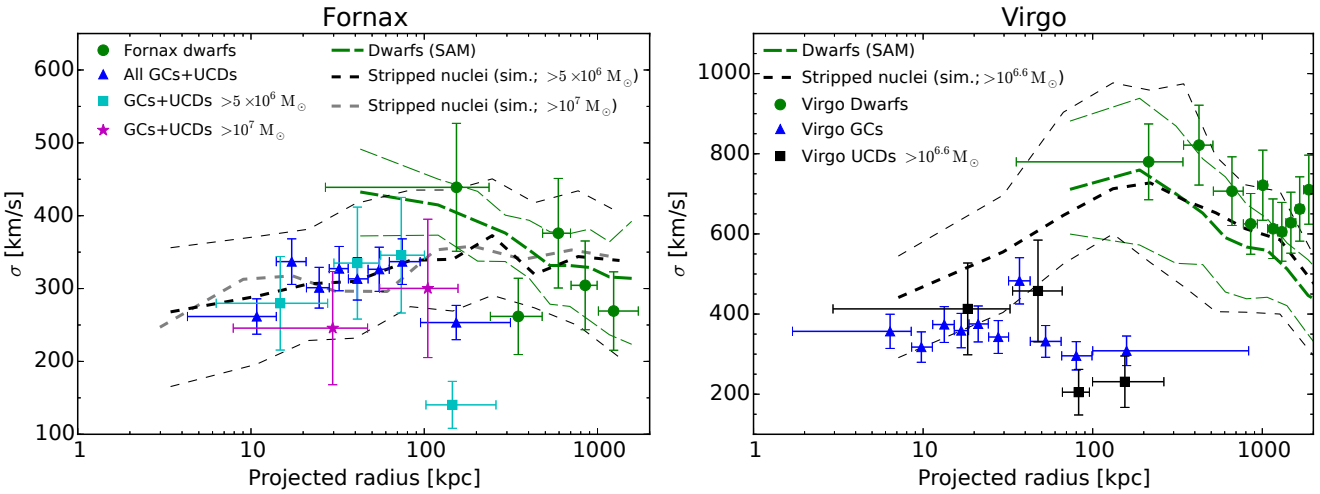

Figure 4. Velocity dispersions σ of simulated stripped nuclei (dashed lines) and dwarf galaxies (long dashed lines) compared with GC and UCD (triangles, squares and stars) and dwarf galaxy (circles) populations in the Fornax (left panel) and Virgo clusters (right panel) as a function of projected radius. The lines for the simulation data are averages of all clusters over three sight-lines (along the x-, y- and z-axes of the simulation) with the standard deviation between individual clusters given by the thin lines (long and short dashes for dwarfs and stripped nuclei, respectively). All observational data is split into bins of equal numbers, where the point for radius is given by the mean of all objects within a bin and the extent of all objects within a bin is shown by the horizontal error bars. For the Fornax cluster GCs+UCDs we show σ for the whole sample (blue triangles), objects with masses $M > 5 \times 10^6\,\mathrm{M}_\odot$ (cyan squares; approximately complete within 83 kpc) and objects with masses $M > 10^7\,\mathrm{M}_\odot$ (magenta stars; approximately complete within 300 kpc). We make the same mass cuts for stripped nuclei as the observed GCs+UCDs (with the black and grey dashed lines for the Fornax cluster showing mass limits of $M > 5 \times 10^6\,\mathrm{M}_\odot$ and $M > 10^7\,\mathrm{M}_\odot$, respectively) but only show the standard deviation of the $M > 5 \times 10^6\,\mathrm{M}_\odot$ limit for clarity. For the Virgo cluster UCDs (defined as having $R_e \gtrsim 10$ pc) and stripped nuclei we only use objects with masses larger than $10^{6.6}\,\mathrm{M}_\odot$ where the observations are approximately complete within 288 kpc. Virgo cluster GCs are from Strader et al. (2011, excluding any objects defined as UCDs). For the observed populations the standard deviations are determined by $\sqrt{N}$ statistics[8].

Throughout this section, to determine M/L ratios for observed GCs and UCDs we use the M05 SSP (rHB) with a Kroupa IMF and 13 Gyr ages as the difference between the 11 and 13 Gyr models is small and the model with a Kroupa IMF is intermediate between the Chabrier and Salpeter IMF SSPs. We caution here that since the velocities of the stripped nuclei are determined by a single particle in the simulations the velocities could be incorrect compared to that expected for a system of particles. Since we are calculating velocity dispersions and not comparing the velocities of individual nuclei we expect this will not affect our results significantly. However the method of determining which galaxies are disrupted in the SAM may severely affect our results (e.g. by choosing galaxies with high relative velocities that may not be disrupted in reality) and therefore caution must be taken when interpreting these results. The simulations were observed from three sight-lines (the x-, y- and z-axes of the simulation) and the data from all clusters were combined for the velocity dispersion measurements to improve statistics.

In the left panel of Fig. 4 we show the predicted velocity dispersions for stripped nuclei and dwarf galaxies from the simulations compared with the velocity dispersions of the Fornax GC+UCD and dwarf galaxy populations. The typical deviation in average stripped nuclei velocity dispersion between individual clusters is ~ 90 km s^{-1} and the stripped nuclei show no change of velocity dispersion with mass. For the dwarf galaxies we take all observed galaxies with $-19.6 < M_B/\mathrm{mag} < -13.4$, corresponding to $10^8 < M_*/\,\mathrm{M}_\odot < 10^{10.5}$ in the simulations assuming a mass-to-light ratio $M/L_B = 3\,(\mathrm{M/L})_\odot$, giving 25 objects per bin. The velocity dispersions of the SAM dwarf galaxies are in good agreement with the observed dwarf galaxies which suggests the cluster virial mass range is accurate. For the Fornax GCs+UCDs we show the whole sample (117 objects per bin), objects with masses $M > 5 \times 10^6\,\mathrm{M}_\odot$ (approximately complete within 83 kpc; 20 objects per bin) and objects with masses $M > 10^7\,\mathrm{M}_\odot$ (approximately complete within 300 kpc; 10 objects per bin). Due to the low number of objects per bin for the GCs+UCDs with masses $> 5 \times 10^6\,\mathrm{M}_\odot$ and $> 10^7\,\mathrm{M}_\odot$ the actual uncertainties are probably larger than shown. There is no significant change in the velocity dispersions of the GCs+UCDs with different mass cuts and is therefore consistent with the whole population originating from the same distribution. The outermost bins (~ 150 kpc) for all GCs+UCDs and $M > 5 \times 10^6\,\mathrm{M}_\odot$ have low velocity dispersions relative to the rest of the population. However the observations are incomplete at this radius and having a complete sample may increase the velocity dispersion measurement.

Interestingly, for the Fornax cluster the predicted velocity dispersions for stripped nuclei agree very well with the observed GCs+UCDs. This may be a consequence of many GCs being accreted from dwarf galaxies by the central cluster galaxy, and thus having a similar origin and ve-

[8] Note that $\sqrt{N}$ statistics leads to underestimated errors of the velocity dispersion if the distribution even slightly deviates from normality (Beers et al. 1990) and therefore the errors are probably underestimated.

locities to stripped nuclei (e.g. Côté, Marzke & West 1998; Hilker, Infante & Richtler 1999b). The stripped nuclei have a velocity dispersion almost constant with radius which agrees with GCs+UCDs at small distances (less than 100 kpc) and dwarf galaxies at large distances (greater than 200 kpc). As found by Gregg et al. (2009), UCDs and stripped nuclei have lower velocity dispersions than dwarf galaxies in the central regions of the Fornax cluster. The difference between dwarfs and stripped nuclei implies there is a bias towards galaxies with low relative velocities (compared to the host galaxy) being disrupted at the centre of galaxy clusters. Given the finding of similar velocity dispersions for GCs and stripped nuclei, velocity dispersions are therefore unable to distinguish between the formation mechanisms of UCDs in the Fornax cluster.

In the right panel of Fig. 4 we show the velocity dispersions of the Virgo GC (70 objects per bin), UCD (14 objects per bin) and dwarf galaxy populations (68 objects per bin) compared with the predictions for stripped nuclei and dwarf galaxies from the simulations. The Virgo GCs are from the sample compiled by Strader et al. (2011), have i-band luminosities between -7.65 and -12.3 mag and are defined as having sizes $\lesssim$ 10 pc. Virgo UCDs are from (Zhang et al. 2015) and are defined as having sizes $\gtrsim$ 10 pc. Again, due to the low number of objects per bin, the actual uncertainties for UCDs are probably much larger than those shown. The typical deviation in average stripped nuclei velocity dispersion between individual clusters is $\sim$ 130 km s^{-1}. For the observed dwarf galaxies from the EVCC we include both certain and possible members. The most distant points for the dwarfs are therefore probably significantly affected by non-cluster members that account for the rise in velocity dispersion. The velocity dispersion profile of the simulated dwarfs is on average slightly lower than the observed dwarfs but is within the cluster-to-cluster scatter of the simulations. Zhang et al. (2015) previously compared Virgo cluster GC and UCD velocity dispersions and found that UCDs have velocity dispersions more similar to blue GCs than red GCs and red GCs have an overall lower velocity dispersion than both blue GCs and UCDs. All three populations have dispersions lower than dwarf elliptical galaxies. Since we include both red and blue GCs the similar velocity dispersions of UCDs and GCs is due to blue GCs outnumbering red GCs by a factor of three in the sample.

For the Virgo cluster the predicted velocity dispersions of stripped nuclei match reasonably well that of the observed UCDs within 60 kpc. For larger distances the stripped nuclei have significantly elevated velocity dispersions compared to the GCs and UCDs and instead trace that of the dwarf galaxies. This could indicate that despite their sizes most Virgo UCDs are simply GCs, however more work is needed on the modelling side before strong conclusions can be made.

The cause of stripped nuclei velocities in Virgo-like clusters (and to a lesser extent, Fornax-like clusters) following that of the dwarf galaxies at distances larger than $\sim$100 kpc is the origin of the objects. In Fig. 5 we show the fraction of 'accreted' stripped nuclei for Fornax- and Virgo-sized clusters. Here accreted refers to stripped nuclei that formed around galaxies other than the central galaxy of the cluster (which may or may not have then been disrupted itself). At distances less than 100 kpc most stripped nuclei ($>$ 70 per cent) form around the central galaxy of the cluster. The accreted fraction then rises sharply and above distances of 200 kpc most stripped nuclei ($>$ 70 per cent) are formed around satellite galaxies (or galaxies which later become satellites). This is very similar to the distance where M87 GCs become contaminated by intra-cluster GCs ($\sim$ 150 kpc, Zhang et al. 2015).

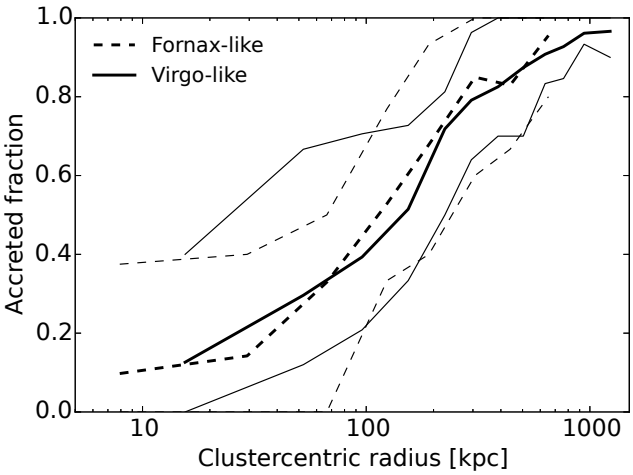

Figure 5. The accreted fraction of simulated stripped nuclei for Fornax- (thick solid line) and Virgo-like clusters (thick dashed line) as a function of clustercentric distance. The mean lines are averages of stripped nuclei in all clusters over three sight-lines (along the x-, y- and z-axes of the simulation) with the standard deviation between individual clusters given by the thin lines.

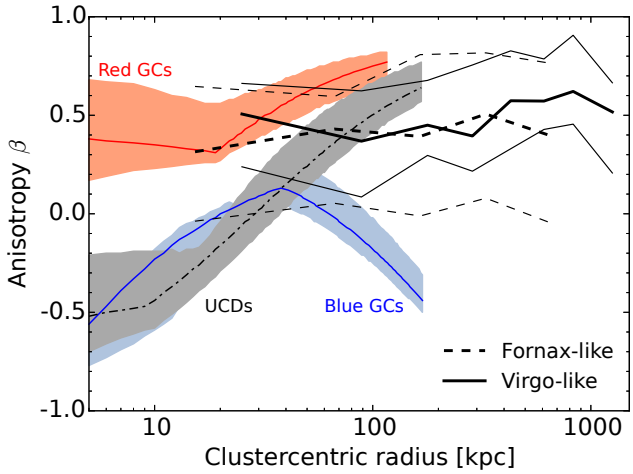

Figure 6. The orbital anisotropy of simulated stripped nuclei for Fornax- (thick solid line) and Virgo-like clusters (thick dashed line) as a function of clustercentric distance. The mean and standard deviations are as in Fig. 5. We also show the anisotropy parameters determined by Zhang et al. (2015) for Virgo cluster blue and red GCs (blue and red lines) and UCDs (black dash-dotted line), with the 1σ confidence regions shown as the shaded areas.

In Fig. 6 we show the orbital anisotropy of stripped nuclei for Fornax- and Virgo-sized clusters. Here we include all stripped nuclei to obtain reliable statistics as anisotropy is independent of mass in our model. As our model does not take into account ongoing mass-loss of stripped nuclei through tidal stripping which would preferentially re-

move objects at small distances with radially biased orbits, at small radii ($\sim$ 10 kpc) the anisotropies measured for the simulations are probably inaccurate. We find the anisotropy of stripped nuclei is preferentially radially biased with no dependency on clustercentric distance, having a typical value of $\beta \sim 0.5$. This agrees well with the anisotropy of Virgo UCDs determined from Jeans analysis (Zhang et al. 2015) at distances of $\gtrsim$ 50 kpc. At smaller radii the simulations strongly disagree with observation, where UCDs have $\beta \sim -0.5$ at 10 kpc, which can be attributed to the lack of ongoing disruption. Zhang et al. also found blue GCs have similar anisotropies to UCDs at distances smaller than 40 kpc, but have $\beta < 0$ at larger distances. This might indicate many UCDs at small distances have an origin similar to blue GCs, with the contribution of stripped nuclei increasing with distance. However our model does not include possible circularization of orbits by dynamical friction or the altering of orbits by major galaxy mergers.

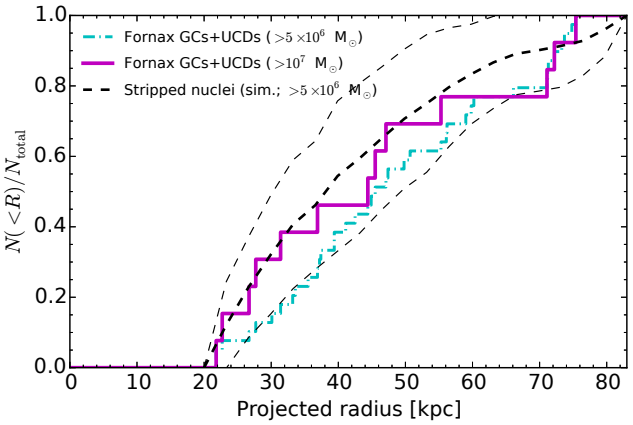

Figure 8. Normalized projected radial distribution of Fornax cluster GCs+UCDs with masses $> 5\times10^6$ M$_\odot$ (dash-dotted cyan line) and $> 10^7$ M$_\odot$ (solid magenta line) and simulated stripped nuclei with masses $> 5 \times 10^6$ M$_\odot$ within 83 kpc (with standard deviation shown by the thin lines).

4.3 Radial distributions

In this section we compare the predicted radial distributions for our model stripped nuclei and dwarf galaxies from the G11 SAM with observations in the Fornax and Virgo clusters. As in the previous section, we use M05 SSP (rHB) with a Kroupa IMF and 13 Gyr ages to determine M/L ratios for the observed GCs and UCDs.

The radial distributions of GCs+UCDs (with masses $> 10^7$ M$_\odot$ where observations are complete) and dwarf galaxies in the Fornax cluster (solid lines) and the predictions from simulations for stripped nuclei and dwarf galaxies (dashed lines) are shown in Fig. 7. Here we include galaxies without radial velocity measurements in the observed dwarf galaxy sample. The innermost 20 kpc is excluded since dwarf galaxy and GC+UCD counts are incomplete due to the high surface brightness of the central galaxy. Assuming an average mass-to-light ratio $M/L_B = 3\,(\mathrm{M/L})_\odot$, the luminosity limits for the observed dwarf galaxies $-19.6 < M_B/\mathrm{mag} < -13.4$ approximately correspond to the mass limits for dwarf galaxies in the simulation $10^8 < M_*/\,\mathrm{M}_\odot < 10^{10.5}$. The average radial distribution of the simulated stripped nuclei is more extended than that of observed GCs+UCDs, although, due to the low number of objects, there is large scatter in the simulations and the normalized distribution agrees with the observations at the $\sim$1-σ level. In Fig. 8 we show the radial distribution of Fornax GCs+UCDs and simulated stripped nuclei within 83 kpc, where we can be confident observations are complete. We don't include in the plot stripped nuclei with masses $> 10^7$ M$_\odot$ since the predictions are same as for the $> 5 \times 10^6$ M$_\odot$ mass cut but with a slightly larger standard deviation. Interestingly within this radius the radial distributions of the GCs+UCDs and stripped nuclei all agree very well and may suggest stripped nuclei formation is too efficient in our model beyond this distance for the most massive progenitor galaxies ($M_* \gtrsim 10^{10}$ M$_\odot$).

Both the numbers and shape of the distribution for dwarf galaxies disagrees strongly between the observations and simulations in Fig. 7. This is in contrast to Weinmann et al. (2011) who found the surface number density profile for Fornax cluster dwarf galaxies is reproduced by the G11 SAM. The difference is due to our fainter mass/luminosity limit for dwarf galaxies compared to Weinmann et al.. The simulations predict 40 per cent more dwarf galaxies than observed and also show a more concentrated distribution than the observations. The overproduction of dwarf galaxies in clusters in the G11 SAM is already well known (G11; Weinmann et al. 2011) and might be due to too efficient star formation in dwarf galaxies, too strong clustering on small scales or inaccurate modelling of tidal effects. As discussed in section 5.2 of P14, the too strong clustering of galaxies at small scales does not affect our predictions since the fraction of mass in a halo that was accreted in subhaloes of a given mass is relatively insensitive to the shape of the power spectrum (Zentner & Bullock 2003; Dooley et al. 2014). Whether a change in the efficiency of star formation will affect our predictions is unclear as changes to a parameter in the SAM may be offset by other factors, although it is unlikely to affect radial distributions. Since tidal effects are strongest in the cluster centre, more accurate modelling of tidal effects may decrease dwarf galaxy numbers and create a more extended radial distribution, thereby increasing the number of stripped nuclei.

In Fig 9 we show the predicted radial distributions of stripped nuclei and dwarf galaxies in Virgo-sized clusters compared with blue and red GCs, UCDs and dwarf galaxies in the Virgo cluster. The observed dwarf galaxy sample is from VCC (Binggeli et al. 1985, excluding probable background galaxies) and includes all galaxies with masses $10^8 < M_*/\,\mathrm{M}_\odot < 10^{10.5}$ (assuming $M/L_B = 3\,(\mathrm{M/L})_\odot$). As for the Fornax cluster the number of dwarf galaxies is overpredicted in the SAM and the radial distribution is too concentrated compared to the observations. The radial distribution of Virgo GCs was determined from the Sérsic profile fits to the red and blue GCs (Zhang et al. 2015). Zhang et al. (2015) previously compared the surface number density profiles of red and blue GCs with UCDs. They found UCDs follow the red GCs at distances larger than 70 kpc (which can also be seen in Fig. 9) and have a profile shallower than both red and blue GCs at smaller distances.

We find the stripped nuclei have a radial distribution that is significantly more extended than the UCDs and red GCs but is only slightly more extended than the blue GCs.

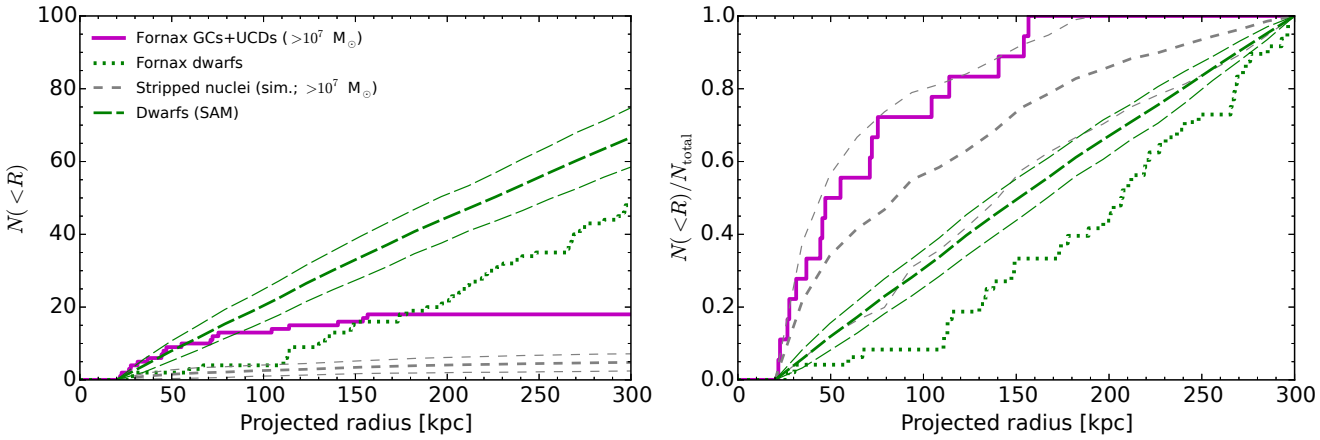

Figure 7. Absolute (left) and normalized (right) projected radial distributions of Fornax cluster GCs+UCDs with masses $> 10^7\,\mathrm{M}_\odot$ (solid magenta line) and dwarf galaxies (with luminosities $-19.6 < M_B/\mathrm{mag} < -13.4$; dotted green line) compared with the predictions of stripped nuclei with stellar masses $M_* > 10^7\,\mathrm{M}_\odot$ (thick grey dashed line) and dwarf galaxies (with stellar masses $10^8 < M_*/\mathrm{M}_\odot < 10^{10.5}$; thick long-dashed green line) from simulations (with standard deviation shown by the thin lines). Each simulated cluster is observed from three directions (x-, y- and z-axes of simulation) and the average radial distribution is used. The innermost 20 kpc is excluded since dwarf galaxy and GC+UCD counts are incomplete due to the high surface brightness of the central galaxy.

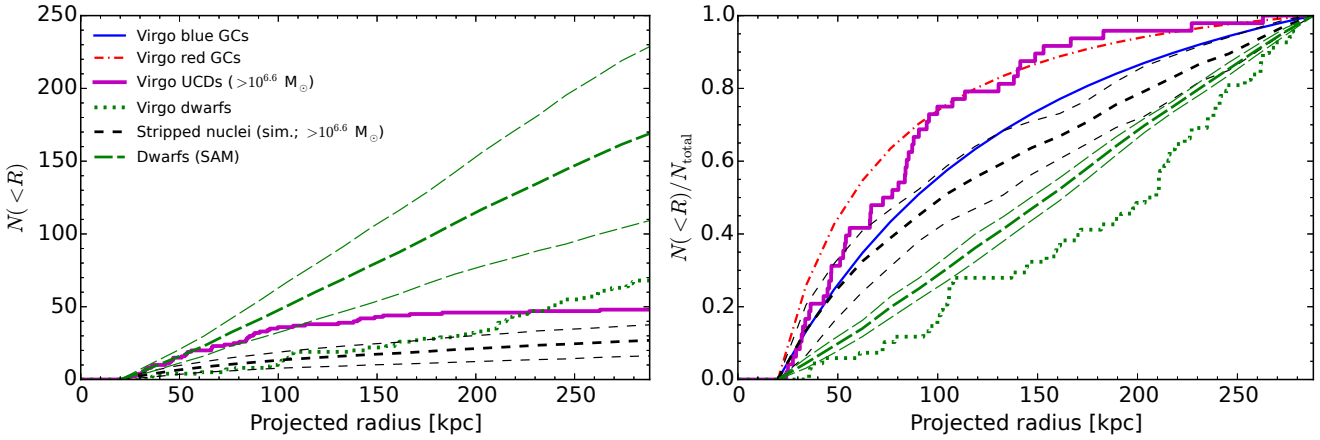

Figure 9. Absolute (left) and normalized (right) projected radial distributions of blue and red GCs (blue thin solid and red dash-dotted lines), UCDs (solid magenta line) and dwarf galaxies in the Virgo cluster (from VCC; dotted green line) within 288 kpc (within which the UCDs are approximately complete) compared with the predictions of stripped nuclei and dwarf galaxies from simulations (black dashed and green long-dashed lines with standard deviation shown by dotted lines). For the Virgo cluster UCDs and stripped nuclei we only use objects with masses larger than $10^{6.6}\,\mathrm{M}_\odot$ where the observations are approximately complete. Each simulated cluster is observed from three directions (x-, y- and z-axes of simulation) and the average radial distribution is used. The innermost 20 kpc is excluded since dwarf galaxy and GC+UCD counts are incomplete due to the high surface brightness of the central galaxy.

This may suggest a common origin of stripped nuclei and blue GCs. However if more efficient disruption of galaxies at the cluster centre (∼100 kpc) was implemented in the G11 SAM to improve dwarf galaxy numbers, stripped nuclei numbers would increase and the radial distribution would become more centrally concentrated.

4.4 Metallicities

In order to compare the predicted metallicities for stripped nuclei with the observed metallicities of UCDs we must assign metallicities to the stripped nuclei. We first determine $\log(\mathrm{Z/Z}_\odot)$ of the progenitor galaxies from the G11 SAM. We then convert to [Fe/H] using the relation $[\mathrm{Z/H}] = [\mathrm{Fe/H}] + 0.94[\alpha/\mathrm{Fe}]$ (Thomas, Maraston, & Bender 2003) and assuming $[\mathrm{Z/H}] = \log(\mathrm{Z/Z}_\odot)$. We assume that $[\alpha/\mathrm{Fe}] = 0.3$ which is typical of GCs, UCDs, bulges and (giant) ellipticals (e.g. Pritzl et al. 2005; Francis et al. 2012; Kuntschner et al. 2010). Nuclear clusters typically have $[\alpha/\mathrm{Fe}] \sim 0$ (Paudel et al. 2011), although there is large scatter with some clusters having $[\alpha/\mathrm{Fe}] \sim 0.5$. However nuclear clusters that can be observed are objects that have survived until the present day with potentially extended star formation histories and therefore may have different properties to nuclear clusters at high redshift. Thus it is plausible that at high redshift (where most stripped nuclei are formed, P14), nuclear clusters have elevated α-abundance ratios due to formation in starbursts or GC infall by dynamical friction. Finally, we assign the nucleus of each galaxy the metallicity of their host galaxy with an offset of 0.067 dex given

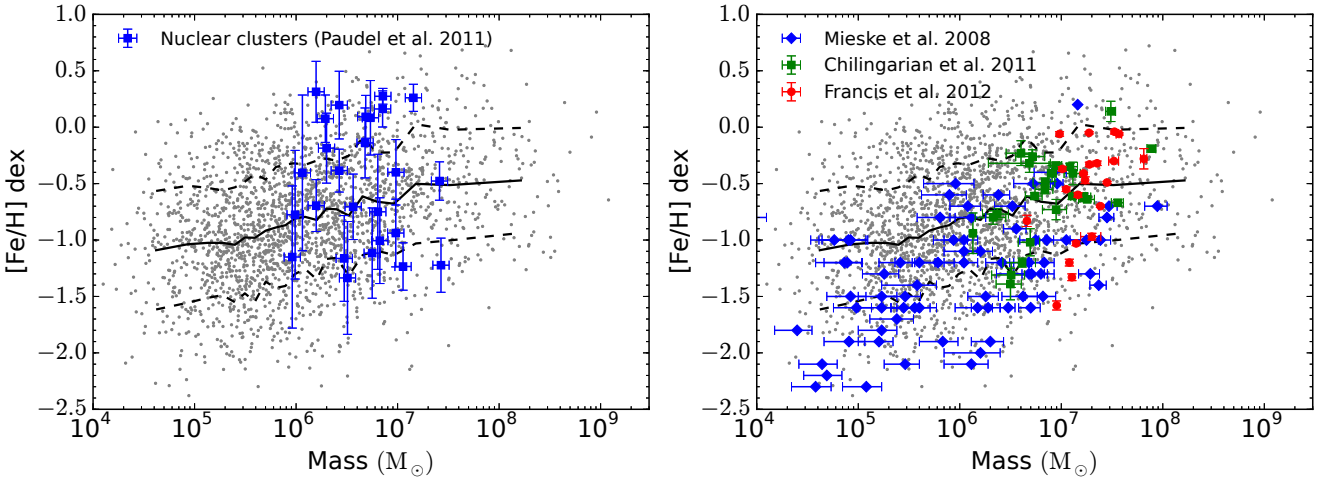

Figure 10. Predicted metallicities of stripped nuclei in Fornax- and Virgo-sized galaxy clusters (grey points) compared with nuclear clusters from Paudel et al. (2011, left panel) and GCs and UCDs from nearby galaxies and galaxy clusters (right panel) from Mieske et al. (2008), Chilingarian et al. (2011) and Francis et al. (2012). The mean and confidence interval for the simulated stripped nuclei are given by the solid and dashed lines, respectively, using bin sizes of 100 objects.

nuclei are typically slightly more metal rich than their host galaxies and for each nucleus add a random offset drawn from a Gaussian of a width 0.46 dex to account for the typical scatter between the metallicity of nuclei and their host galaxies (Paudel et al. 2011). In the left panel of Fig. 10 we show the metallicities predicted for the stripped nuclei compared with the nuclear clusters from Paudel et al. (2011). To convert to stellar masses, SDSS r-band M/L ratios for the nuclear clusters were determined from their ages and metallicities with the closest fit M05 models (Kroupa IMF, red horizontal branch) from their SSP grid in age and metallicity. The metallicities we predict for the stripped nuclei are in reasonable agreement with the nuclear cluster metallicities, although within the same mass range the nuclear clusters are 0.2 dex more metal rich on average.

We show the predicted metallicities for stripped nuclei compared to the metallicities of GCs and UCDs (see Section 3.3) in the right panel of Fig. 10. Where possible we use the dynamical masses measured for objects in this sample. For masses $\gtrsim 5 \times 10^6$ M$_\odot$ there is good agreement between the metallicities predicted for stripped nuclei and those of the observed GCs+UCDs, although the stripped nuclei reach larger metallicities. Below masses of 10^6 M$_\odot$ the stripped nuclei are predicted to be 0.5 dex more metal rich on average than the observed GCs. This is expected because many blue (i.e. metal-poor) genuine GCs mix into the sample for masses below 10^7 M$_\odot$ due to the mass-metallicity relation (the blue tilt) for masses above 2×10^6 M$_\odot$ (e.g. Norris & Kannappan 2011). However if nuclear clusters are mostly formed from infall of (primarily metal-poor) star clusters via dynamical friction in low-mass galaxies and star formation following gas accretion in high-mass galaxies (e.g. Turner et al. 2012) the metallicity offset between nuclear clusters and their host galaxies may change with galaxy mass, causing stripped nuclei from low-mass galaxies to be more metal-poor.

To compare in more detail the predictions for metallicities of stripped nuclei with those observed for GCs and UCDs, in Fig. 11 we show the normalized histogram of GCs and UCDs and simulated stripped nuclei with masses between $10^7 < M/\,\mathrm{M}_\odot < 10^8$ for objects from Fig. 10. The simulation histogram shows the mean of 100 repeated metallicity assignments for the stripped nuclei to account for the randomly chosen metallicity offsets between galaxies and nuclear clusters. We find reasonable agreement between the predictions and the observations given we have not tried to mimic the fraction of objects coming from different galaxy clusters. The four outermost bins of the simulation histogram objects show some deviation from the observed objects. However, due to the low number of stripped nuclei in each simulated galaxy cluster, the standard deviation for individual clusters is much larger than the standard deviation of the mean for all galaxy clusters and may account for this

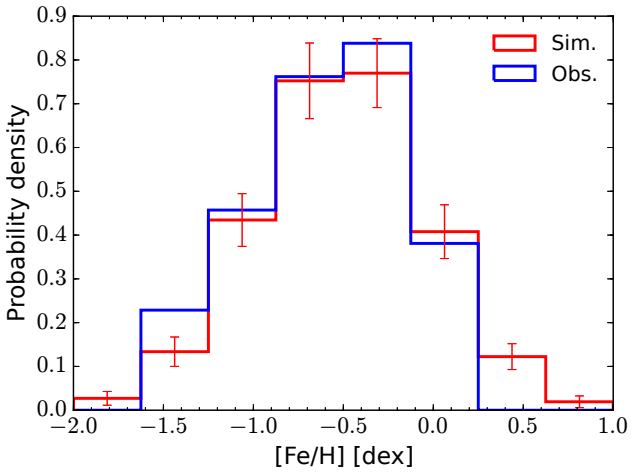

Figure 11. Normalized histogram (such that the integral under the histogram is 1) of the metallicities of observed GCs and UCDs (Obs.) and simulated stripped nuclei (Sim.) from Fig. 10 with masses between $10^7 < M/\,\mathrm{M}_\odot < 10^8$. Calculations for the simulations were repeated 100 times to account for the randomly chosen metallicity offsets between galaxies and nuclear clusters with the histogram and error bars showing the mean and standard deviation for each repeat over all galaxy clusters.

difference. According to a KS test, the observed GCs and UCDs show a 25 per cent probability of being drawn from the same distribution as the stripped nuclei (the average in log-space of 100 repeated calculations, with a standard deviation of 0.5 dex). This shows that many of the most massive UCDs could have formed from the tidal stripping of nucleated galaxies. However, given the trend in [Fe/H] with mass for the observed GCs and UCDs (below masses of $10^7\,\mathrm{M}_\odot$ where we find stripped nuclei contribute little to the population, Section 4.1), the possibility of the most massive objects being the high-mass end of the GC population is also not ruled out by metallicity.

4.5 Central black holes

UCDs are known to have dynamical mass-to-light ratios above what is expected from their stellar populations (Haşegan et al. 2005; Mieske et al. 2008, 2013). One suggestion is that these elevated mass-to-light ratios are caused by UCDs harbouring central intermediate mass black holes (IMBH) or SMBHs (Mieske et al. 2013). The finding of the first UCD to contain a SMBH (M60-UCD1, Seth et al. 2014) gives plausibility to the possibility that many UCDs may host black holes (although interestingly the dynamical mass of M60-UCD1 is consistent with the stellar mass predicted from population synthesis models, Strader et al. 2013).

In the left panel of Fig. 12 we show the predicted masses of central black holes for stripped nuclei progenitor galaxies in the G11 SAM. In the right panel we show the predicted masses of central black holes in stripped nuclei, where the black hole masses are taken from the progenitor galaxies of the stripped nuclei in the SAM. According to the model, the fraction of stripped nuclei with a central black hole is 97 per cent. For Fornax-like clusters we predict that stripped nuclei host 13 ± 5 black holes more massive than $10^6\,\mathrm{M}_\odot$ and 3 ± 2 black holes more massive than $10^7\,\mathrm{M}_\odot$. For Virgo-like clusters we predict that stripped nuclei host 59 ± 6 black holes more massive than $10^6\,\mathrm{M}_\odot$ and 14 ± 2 black holes more massive than $10^7\,\mathrm{M}_\odot$. In the model, black holes form during gas-rich mergers and thereafter grow either by the merger of black holes or the accretion of cold or hot gas ('quasar' and 'radio' mode, respectively). At low galaxy masses the black hole masses are dependent on the simulation resolution and the method in which black holes are first seeded. Black hole masses in galaxies with stellar masses less than $\sim 10^9\,\mathrm{M}_\odot$ (and thus stripped nuclei masses less than $\sim 10^{6.5}\,\mathrm{M}_\odot$) can therefore be considered very uncertain.

In Fig. 12 we also show M60-UCD1 (the first UCD to have a confirmed central black hole, Seth et al. 2014), the implied black hole masses of UCDs assuming their elevated dynamical mass-to-light ratios are due to central black holes (Mieske et al. 2013) and the limits for central black holes in the GCs ω Cen and G1 (Lützgendorf et al. 2013; both of which are thought to be stripped nuclei, e.g. Hilker & Richtler 2000, Meylan et al. 2001). The black hole mass of M60-UCD1 agrees well with the predictions for stripped nuclei and progenitor galaxies, falling within the 1σ confidence intervals. There is also remarkable agreement between the simulations and the inferred black hole masses of UCDs from Mieske et al. (2013). For UCDs with an implied black hole mass above zero, 74 per cent (23/31) of the data points fall within the 1σ confidence interval of the simulation predictions. For UCDs with a lower black hole mass limit above zero, 79 per cent (15/19) of the data points fall within the 1σ confidence interval of the simulation predictions. The GCs ω Cen and G1 both have black hole limits well below the mean predicted for their mass by the model, but are within the overall scatter of the simulated objects.

5 DISCUSSION

5.1 The origin of UCDs

Two main scenarios have been suggested for the formation of UCDs: they are the high-mass end of the GC mass function observed around galaxies with rich GC systems (Mieske et al. 2002, 2012) or the nuclei of tidally stripped dwarf galaxies (Bekki et al. 2001, 2003; Drinkwater et al. 2003; Pfeffer & Baumgardt 2013). Although the internal properties (e.g. metallicities) of simulated UCDs formed by tidal stripping generally agree well with that of observed UCDs, we find tidal stripping cannot be the dominant formation mechanism of UCDs. Instead we suggest most UCDs are simply the high-mass end of the GC mass function with the contribution of UCDs formed by tidal stripping increasing towards higher masses. Above masses of $10^{7.3}\,\mathrm{M}_\odot$, UCDs are consistent with being entirely formed by tidal stripping. In fact for the Virgo cluster more stripped nuclei are predicted than observed UCDs by a factor of 1.5 above this mass.

It has been suggested that size and not mass differentiates between UCDs and GCs (e.g. Zhang et al. 2015). However we find that stripped nuclei cannot account for all Virgo cluster UCDs (which are defined to have sizes $\gtrsim 10$ pc). N-body simulations of the formation of stripped nuclei also show that for pericentre distances $\lesssim 5$ kpc (depending on the progenitor galaxy properties) the stripped nuclei formed will have sizes < 10 pc (Pfeffer & Baumgardt 2013). Thus even for sizes above 10 pc GCs must make a significant contribution and size alone does not discriminate between different formation channels.

These findings are consistent with the findings of other recent studies. Mieske et al. (2012) calculated the fraction of GCs that contribute to the UCD population based on the specific frequencies of GCs around galaxies and found less than 50 per cent of UCDs can have formed by tidal stripping. Mieske et al. (2013) investigated the dynamical-to-stellar mass ratios $\Psi = M_\mathrm{dyn}/M_*$ of UCDs and found evidence for a bimodal distribution, with one population having $\Psi < 1$ similar to GCs and the other having $\Psi > 1$ (see their figures 2 and 3). In the Fornax cluster less than 10 per cent ($17/\sim 200$) of GCs+UCDs with masses $> 2 \times 10^6\,\mathrm{M}_\odot$ have measured dynamical mass-to-light ratios. Of these objects, 9 have $\Psi < 1$ and are thus consistent with being genuine GCs, while 5 have $\Psi > 1$ at the 1σ level and require some additional dark mass. The remaining 3 might be either genuine GCs or UCDs formed by tidal stripping that do not host central black holes (the occupation fraction of supermassive black holes in UCD progenitor galaxies is likely not 100 per cent). In fact the only Fornax UCD with spatially resolved kinematics (UCD3, Frank et al. 2011) has a dynamical mass consistent with the mass predicted from stellar population modelling (Mieske et al. 2013). As we find about 20 UCDs

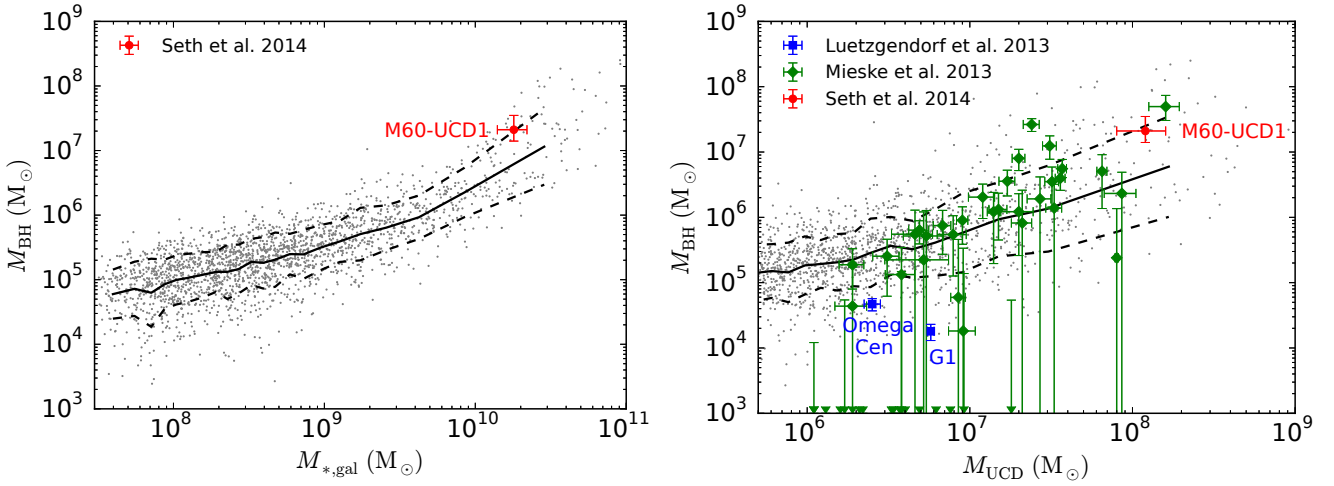

Figure 12. Predicted masses of central black holes in stripped nuclei and their progenitor galaxy mass. The left panel plots against maximum progenitor galaxy stellar mass and the right panel compares against stripped nucleus mass. The mean and 1σ confidence interval for the simulations are given by the solid and dashed lines, respectively, using bin sizes of 100 objects. The typical 1σ confidence interval in $M_{\rm BH}$ is 0.5 dex. For comparison, in the left panel we show the black hole mass of M60-UCD1 against the estimated progenitor bulge mass (Seth et al. 2014) and in the right panel we show the black hole mass of M60-UCD1 (Seth et al. 2014), the inferred black hole masses of UCDs assuming elevated mass-to-light ratios are due to central black holes (Mieske et al. 2013) and the limits for central black holes in the GCs ω Cen and G1 (Lützgendorf et al. 2013). For the observed UCDs and GCs, objects with implied black hole masses of zero are given by triangles at the bottom of the figure.

more massive than 2×10^6 M$_\odot$ will have formed by tidal stripping in the Fornax cluster within 300 kpc (Fig. 2), we expect most of the GC+UCD population without measured dynamical mass-to-light ratios should not have an elevated Ψ if this scenario is correct. Therefore a combination of genuine GCs (where the most massive GCs may have formed in starbursts in the early universe similar to young massive clusters, e.g. Renaud et al. 2015) and stripped nuclear clusters is currently sufficient to explain the properties of all observed UCDs in the Fornax cluster.

If UCDs that formed by tidal stripping of nucleated galaxies host central black holes, they may make a significant contribution to the number of SMBHs in galaxy clusters. Seth et al. (2014) found there are 45 galaxies in Fornax with stellar masses above 3×10^9 M$_\odot$ (where SMBH occupation fraction is high) that are likely to host SMBHs. We predict for Fornax-like clusters that 14 ± 4 stripped nuclei with progenitor galaxy stellar masses larger than 3×10^9 M$_\odot$ may host central black holes. This would increase the number of black holes in the Fornax cluster by ~ 30 per cent. For Virgo-like clusters we predict 60 ± 2 stripped nuclei with progenitor galaxy stellar masses larger than 3×10^9 M$_\odot$ may host central black holes.

The combination of velocity dispersions (σ), anisotropy (β) and radial distributions also points to many UCDs simply being GCs. However we find conflicting results as to whether the contribution of stripped nuclei should be largest at the centre of the cluster or at increasing radii. Zhang et al. (2015) found Virgo UCDs have $\beta \sim -0.5$ at < 10 kpc, increasing to 0.5 at > 100 kpc, and an anisotropy profile similar to blue GCs < 40 kpc. In contrast to the UCDs, at radii larger than 40 kpc blue GCs have a tangentially biased anisotropy profile. We predict stripped nuclei have $\beta \sim 0.5$ at all radii (Fig. 6). This points to stripped nuclei contributing more with increasing radius. However effects not included in our model (circularization of orbits by dynamical friction, continuous tidal stripping removing objects on very radial orbits or major galaxy mergers altering the orbits of the innermost objects) might account for the tangentially biased orbits at the cluster centre. On the other hand, stripped nuclei match the UCD velocity dispersions at the centre of clusters but not at distances larger than 50-100 kpc where σ increases to match that of dwarf galaxies (Fig. 4), which points to stripped nuclei contributing more at the cluster centre. Similar to the velocity dispersions, the predicted stripped nuclei radial distributions match UCDs within $\sim$100 kpc but not at larger radii. This may be related to the overabundance of dwarf galaxies predicted by the G11 SAM at cluster centres (Fig. 7 and 9) and if more realistic galaxy disruption was implemented may increase the number of stripped nuclei at the cluster centre and create a more concentrated radial distribution. For the observed Virgo UCDs, the radially biased anisotropy and low velocity dispersion at distances of 100-200 kpc implies the number density distribution has to drop very strongly beyond these distances. This is in disagreement with the prediction for stripped nuclei where velocity dispersions increase at distances $\gtrsim 100$ kpc due to the increasing contribution of stripped nuclei formed around satellite galaxies and for which there is no strong drop in number density.

The predicted velocity dispersions of stripped nuclei also has important implications for the origin of blue GCs in galaxy clusters. Blue GCs that were accreted from dwarf galaxies should have similar velocity dispersions and orbital anisotropy to stripped nuclei, i.e. σ that follows dwarf galaxies at distances larger than 100 kpc and $\beta \sim 0.5$. The blue GCs around M87 have $\sigma \sim 450$ km s^{-1} at 200 kpc and a tangentially biased anisotropy (Zhang et al. 2015) which suggests a significant fraction of blue GCs could not have been accreted from dwarf galaxies around M87. Unless their

orbits were significantly changed after accretion, this would imply most blue GCs were either formed in situ in the halo of M87 or possibly accreted during major mergers.

It is not clear how to reconcile the conflicting results for velocity dispersions and anisotropies with the current data. However it might imply the UCD populations are dominated by GCs and that we are not comparing objects with similar formation histories. The predicted mass function for stripped nuclei suggests the most massive UCDs have the best chance of being 'genuine UCDs' (i.e. the nuclear star clusters of tidally stripped galaxies). However the number of such objects is not large enough to make statistically significant comparisons. Distinguishing between the formation mechanisms of individual UCDs may therefore only be possible through the presence of central black holes (Seth et al. 2014), recent star formation (Norris & Kannappan 2011; Norris et al. 2015) or extended, massive tidal features of their disrupting progenitor galaxy (Amorisco et al. 2015; Mihos et al. 2015; Voggel et al. 2015).

5.2 Future work

More work is needed on both the observation and simulation sides to further constrain the stripped nuclei scenario (and indeed the formation of UCDs generally). In nearby galaxy clusters, complete, spectroscopically confirmed samples of GCs and UCDs to larger clustercentric radii would enable better comparisons. Studies of different galaxy clusters have used different criteria to differentiate between GCs and UCDs; interpreting these results is difficult as different methods may obtain different results within the same cluster. Future work should investigate each galaxy cluster using consistent methods to enable comparison between clusters. Comparisons between observed and model UCD populations should be extended beyond the central galaxy of a galaxy cluster. Programs like the NGVS (Ferrarese et al. 2012; Zhang et al. 2015) combined with further spectroscopic surveys will enable a systematic comparison over the main subclusters of a galaxy cluster. Observational constraints on the SMBH occupation fraction in nucleated dwarf galaxies can be used to determine what fraction of stripped nuclei (and thus UCDs) should have elevated dynamical mass-to-light ratios due to the presence of central black holes and, together with more observations of UCD dynamical mass-to-light ratios, determine if central black holes alone are sufficient to explain UCDs with elevated mass-to-light ratios.

On the simulation side a number of further refinements of our model are needed. Too many high-mass stripped nuclei are predicted for the Virgo cluster (this may also be the case for the Fornax cluster, however the number of objects is very small). A number of possible explanations exist for this difference:

(i) The galaxy disruption criterion in the SAM is unrealistic. According to the SAM, galaxies are disrupted when the density of a satellite galaxy within its half-mass radius is less than the host halo density at pericentre. This might overestimate the disruption of the highest mass stripped nuclei progenitor galaxies ($M_* \sim 10^{10.5}$-$10^{11}\,\mathrm{M}_\odot$) since such objects would need to lose more than 99 per cent of their mass to become UCDs.

(ii) Related to the previous point, the high-mass stripped nuclei might not be observed as UCDs but instead as compact ellipticals. If disruption of the progenitor galaxy is incomplete (which is especially important for the highest mass progenitor galaxies that may require extremely small pericentre passages to completely remove the galaxy) the resulting object may have a size larger than 100 pc and should be considered a compact elliptical rather than a UCD.

(iii) Our assumption that nuclei have a constant fraction of galaxy mass at all redshifts may not be realistic.

Future stripped nucleus formation models should include more realistic models for galaxy disruption, circularization of orbits by dynamical friction, continuous tidal stripping of the stripped nuclei and the effect of major galaxy mergers on stripped nuclei orbits. As the build up of nuclear clusters with redshift is not possible to observe, models of nucleus formation are needed to include physically motivated nuclear cluster formation. Size predictions are also needed to allow for better comparisons, in particular with Virgo cluster UCDs, and to determine if the most massive stripped nuclei predicted should be included in comparisons against UCDs. These changes may affect the predictions for mass function, velocity dispersions and radial distributions.

6 SUMMARY

In this paper we compared in detail the predictions of the semi-analytic model for stripped nucleus formation presented in P14 with the observed properties of UCDs in the local universe. Our main findings are as follows.

(i) The number of stripped nuclei predicted at the high-mass end of the mass function in Fornax-like clusters is consistent with the most massive objects observed. For masses larger than $10^7\,\mathrm{M}_\odot$ we predict stripped nuclei account for $\sim$40 per cent of GCs+UCDs and for masses between 10^6 and $10^7\,\mathrm{M}_\odot$ account for $\sim$2.5 per cent of GCs+UCDs. For the Virgo cluster more high-mass stripped nuclei are predicted than the number of observed UCDs above masses $\sim 10^{7.4}\,\mathrm{M}_\odot$. Below masses of $\sim 10^{6.7}\,\mathrm{M}_\odot$ more Virgo UCDs (defined as having $R_e \gtrsim 10$ pc) are observed than the predicted number of stripped nuclei.

(ii) The excess number of Fornax GCs+UCDs above the GC luminosity function agrees very well with the predicted number of stripped nuclei. Therefore the GC+UCD mass function is consistent with being a combination of stripped nuclei and genuine GCs (formed through the same process as the majority of GCs). This suggests the most massive genuine GC in the Fornax cluster has a mass of $\sim 10^{7.3}\,\mathrm{M}_\odot$.

(iii) The predicted velocity dispersions for stripped nuclei in Fornax-sized clusters agrees well with the observed GC+UCD population at projected distances less than 100 kpc. For the Virgo cluster the velocity dispersions of stripped nuclei agree reasonably well with GCs and UCDs at distances less than $\sim$50 kpc. At larger distances the velocity dispersions of stripped nuclei increase to that of the dwarf galaxies due to the increasing contribution of stripped nuclei accreted satellite galaxies. For both the Fornax and Virgo clusters the velocity dispersions of dwarf galaxies in the G11 SAM agree well with observed dwarf galaxies.

(iv) Stripped nuclei are predicted to have radially biased anisotropies that are approximately constant with radius

($\beta \sim 0.5$). This agrees with Virgo UCDs at distances larger than 100 kpc but disagrees at smaller distances where UCDs have β decreasing to -0.5 at distances less than 10 kpc (Zhang et al. 2015). However, ongoing disruption is not included in our model which would cause orbits to become tangentially biased at small radii.

(v) For Fornax-sized clusters the radial distribution of stripped nuclei agrees well with observed GCs+UCDs within 83 kpc for masses $>5 \times 10^6\,M_\odot$. Within 300 kpc and for masses $>10^7\,M_\odot$ stripped nuclei are on average more extended than observed GCs+UCDs, but consistent due to the large scatter for the simulations. For Virgo-sized clusters the radial distribution of stripped nuclei is significantly more extended than that of UCDs.

(vi) For masses between 10^7 and $10^8\,M_\odot$, the predicted metallicities of stripped nuclei agree well with the observed metallicities of GCs and UCDs. Below masses of $10^6\,M_\odot$, stripped nuclei are predicted to be $\sim$0.5 dex more metal-rich on average than observed GCs and UCDs. This may be due to a metallicity offset between nuclear clusters and host galaxies that scales with galaxy mass.

(vii) The predicted central black hole masses for stripped nuclei agree well with the observed black hole mass of M60-UCD1 and the black hole masses implied for UCDs assuming their elevated mass-to-light ratios are due to central black holes. However, assuming Milky Way GCs with possible central black holes formed as stripped nuclei, the predictions from the modelling are 10-100 time higher than the observed values, suggesting the modelling is inaccurate at these masses or that MW GCs with IMBH estimates are not stripped nuclei. UCD black hole masses may therefore provide another approach to test SMBH formation scenarios.

These findings together suggest that, although not the dominant mechanism of UCD formation, a significant fraction of the highest mass UCDs ($M > 10^7\,M_\odot$) were formed by tidal stripping of nucleated galaxies.

ACKNOWLEDGEMENTS

We thank the anonymous referee for helpful comments and Hong-Xin Zhang for providing us with data for Virgo cluster GCs and UCDs. HB is supported by the Discovery Project grant DP110102608. The Millennium-II Simulation databases used in this paper and the web application providing online access to them were constructed as part of the activities of the German Astrophysical Virtual Observatory (GAVO).

REFERENCES

Adamo A., Kruijssen J. M. D., Bastian N., Silva-Villa E., Ryon J., 2015, MNRAS, 452, 246
Amorisco N. C., Martinez-Delgado D., Schedler J., 2015, preprint (arXiv:1504.03697)
Bassino L. P., Faifer F. R., Forte J. C., Dirsch B., Richtler T., Geisler D., Schuberth Y., 2006, A&A, 451, 789
Baumgardt H., Makino J., 2003, MNRAS, 340, 227
Beers T. C., Flynn K., Gebhardt K., 1990, AJ, 100, 32
Bekki K., Couch W. J., Drinkwater M. J., 2001, ApJ, 552, L105
Bekki K., Couch W. J., Drinkwater M. J., Shioya Y., 2003, MNRAS, 344, 399
Bell E. F., McIntosh D. H., Katz N., Weinberg M. D., 2003, ApJS, 149, 289
Bergond G., et al., 2007, A&A, 464, L21
Binggeli B., Sandage A., Tammann G. A., 1985, AJ, 90, 1681
Binney J., Tremaine S., 1987, Galactic Dynamics. Princeton Univ. Press, Princeton
Blakeslee J. P., et al., 2009, ApJ, 694, 556
Boylan-Kolchin M., Springel V., White S. D. M., Jenkins A., Lemson G., 2009, MNRAS, 398, 1150
Brodie J. P., Romanowsky A. J., Strader J., Forbes D. A., 2011, AJ, 142, 199
Brüns R. C., Kroupa P., 2012, A&A, 547, A65
Bruzual G., Charlot S., 2003, MNRAS, 344, 1000
Chabrier G., 2003, PASP, 115, 763
Chiboucas K., Tully R. B., Marzke R. O., Trentham N., Ferguson H. C., Hammer D., Carter D., Khosroshahi H., 2010, ApJ, 723, 251
Chilingarian I. V., 2009, MNRAS, 394, 1229
Chilingarian I. V., Mieske S., Hilker M., Infante L., 2011, MNRAS, 412, 1627
Côté P., Marzke R. O., West M. J., 1998, ApJ, 501, 554
Côté P. et al., 2006, ApJS, 165, 57
Dabringhausen J., Hilker M., Kroupa P., 2008, MNRAS, 386, 864
Dabringhausen J., Kroupa P., Baumgardt H., 2009, MNRAS, 394, 1529
Dabringhausen J., Kroupa P., Pflamm- Altenburg J., Mieske S., 2012, ApJ, 747, 72
Da Rocha C., Mieske S., Georgiev I. Y., Hilker M., Ziegler B. L., Mendes de Oliveira C., 2011, A&A, 525, A86
Dirsch B., Richtler T., Geisler D., Forte J. C., Bassino L. P., Gieren W. P., 2003, AJ, 125, 1908
Dooley G. A., Griffen B. F., Zukin P., Ji A. P., Vogelsberger M., Hernquist L. E., Frebel A., 2014, ApJ, 786, 50
Drinkwater M. J., Jones J. B., Gregg M. D., Phillipps S., 2000, PASA, 17, 227
Drinkwater M. J., Gregg M. D., Colless M., 2001, ApJ, 548, L139
Drinkwater M. J., Gregg M. D., Hilker M., Bekki K., Couch W. J., Ferguson H. C., Jones J. B., Phillipps S., 2003, Nature, 423, 519
Durrell P. R., et al., 2014, ApJ, 794, 103
Evstigneeva E. A., Gregg M. D., Drinkwater M. J., Hilker M., 2007, AJ, 133, 1722
Ferguson H. C., 1989, AJ, 98, 367
Ferrarese L., et al., 2000, ApJ, 529, 745
Ferrarese L., et al., 2012, ApJS, 200, 4
Firth P., Drinkwater M. J., Evstigneeva E. A., Gregg M. D., Karick A. M., Jones J. B., Phillipps S., 2007, MNRAS, 382, 1342
Firth P., Drinkwater M. J., Karick A. M., 2008, MNRAS, 389, 1539
Francis K. J., Drinkwater M. J., Chilingarian I. V., Bolt A. M., Firth P., 2012, MNRAS, 425, 325
Frank M. J., Hilker M., Mieske S., Baumgardt H., Grebel E. K., Infante L., 2011, MNRAS, 414, L70
Freedman W. L., et al., 2001, ApJ, 553, 47

Gallazzi A., Charlot S., Brinchmann J., White S. D. M., Tremonti C. A., 2005, MNRAS, 362, 41
Georgiev I. Y., Böker T., Leigh N., Lützgendorf N., Neumayer N., 2016, MNRAS, 457, 2122
Genzel R., et al., 2011, ApJ, 733, 101
Goerdt T., Moore B., Kazantzidis S., Kaufmann T., Macciò A. V., Stadel J., 2008, MNRAS, 385, 2136
Graham A. W., Spitler L. R., 2009, MNRAS, 397, 2148
Gregg M. D., et al., 2009, AJ, 137, 498
Guo Q. et al., 2011, MNRAS, 413, 101
Guo Q., White S., Angulo R. E., Henriques B., Lemson G., Boylan-Kolchin M., Thomas P., Short C., 2013, MNRAS, 428, 1351
Hau G. K. T., Spitler L. R., Forbes D. A., Proctor R. N., Strader J., Mendel J. T., Brodie J. P., Harris W. E., 2009, MNRAS, 394, L97
Haşegan M. et al., 2005, ApJ, 627, 203
Hilker M., 2009, in Röser S., ed., Rev. Modern Astron. Vol. 21, Formation and evolution of cosmic structures. Wiley-VCH, Weinheim, p. 199
Hilker M., Richtler T., 2000, A&A, 362, 895
Hilker M., Infante L., Vieira G., Kissler-Patig M., Richtler T., 1999a, A&AS, 134, 75
Hilker M., Infante L., Richtler T., 1999b, A&AS, 138, 55
Hilker M., Baumgardt H., Infante L., Drinkwater M., Evstigneeva E., Gregg M., 2007, A&A, 463, 119
Jerjen H., Tully B., Trentham N., 2004, PASA, 21, 356
Jones J. B. et al., 2006, AJ, 131, 312
Jordán A., et al., 2009, ApJS, 180, 54
Kim S., et al., 2014, ApJS, 215, 22
Kirby E. N., Cohen J. G., Guhathakurta P., Cheng L., Bullock J. S., Gallazzi A., 2013, ApJ, 779, 102
Kroupa P., 2001, MNRAS, 322, 231
Kruijssen J. M. D., 2014, Class. Quantum Gravity, 31, 244006
Kuntschner H., et al., 2010, MNRAS, 408, 97
Lemson G., Virgo Consortium t., 2006, preprint (arXiv:0608019)
Lützgendorf N., et al., 2013, A&A, 555, A26
Marín-Franch A., et al., 2009, ApJ, 694, 1498
Maraston C., Bastian N., Saglia R. P., Kissler-Patig M., Schweizer F., Goudfrooij P., 2004, A&A, 416, 467
Maraston C., 2005, MNRAS, 362, 799
McLaughlin D. E., 1999, ApJ, 512, L9
McLaughlin D. E., van der Marel R. P., 2005, ApJS, 161, 304
Mei S., et al., 2007, ApJ, 655, 144
Meylan G., Sarajedini A., Jablonka P., Djorgovski S. G., Bridges T., Rich R. M., 2001, AJ, 122, 830
Mieske S., Hilker M., Infante L., 2002, A&A, 383, 823
Mieske S., Hilker M., Infante L., 2004a, A&A, 418, 445
Mieske S. et al., 2004b, AJ, 128, 1529
Mieske S., Hilker M., Infante L., Jordán A., 2006, AJ, 131, 2442
Mieske S., Hilker M., Jordán A., Infante L., Kissler-Patig M., 2007, A&A, 472, 111
Mieske S. et al., 2008, A&A, 487, 921
Mieske S., Hilker M., Misgeld I., 2012, A&A, 537, A3
Mieske S., Frank M. J., Baumgardt H., Lützgendorf N., Neumayer N., Hilker M., 2013, A&A, 558, A14
Mihos J. C., et al., 2015, ApJ, 809, L21
Misgeld I., Hilker M., 2011, MNRAS, 414, 3699
Misgeld I., Mieske S., Hilker M., Richtler T., Georgiev I. Y., Schuberth Y., 2011, A&A, 531, A4
Norris M. A., Kannappan S. J., 2011, MNRAS, 414, 739
Norris M. A., et al., 2014, MNRAS, 443, 1151
Norris M. A., Escudero C. G., Faifer F. R., Kannappan S. J., Forte J. C., van den Bosch R. C. E., 2015, MNRAS, 451, 3615
Paudel S., Lisker T., Kuntschner H., 2011, MNRAS, 413, 1764
Paust N. E. Q., et al., 2010, AJ, 139, 476
Peng E. W., et al., 2006, ApJ, 639, 838
Penny S. J., Forbes D. A., Conselice C. J., 2012, MNRAS, 422, 885
Pfeffer J., Baumgardt H., 2013, MNRAS, 433, 1997
Pfeffer J., Griffen B. F., Baumgardt H., Hilker M., 2014, MNRAS, 444, 3670
Phillipps S., Drinkwater M. J., Gregg M. D., Jones J. B., 2001, ApJ, 560, 201
Phillipps S., Young A. J., Drinkwater M. J., Gregg M. D., Karick A., 2013, MNRAS, 433, 1444
Price J., et al., 2009, MNRAS, 397, 1816
Pritzl B. J., Venn K. A., Irwin M., 2005, AJ, 130, 2140
Rejkuba M., Dubath P., Minniti D., Meylan G., 2007, A&A, 469, 147
Renaud F., Bournaud F., Duc P.-A., 2015, MNRAS, 446, 2038
Romanowsky A. J., Strader J., Spitler L. R., Johnson R., Brodie J. P., Forbes D. A., Ponman T., 2009, AJ, 137, 4956
Salpeter E. E., 1955, ApJ, 121, 161
Schuberth Y., Richtler T., Hilker M., Dirsch B., Bassino L. P., Romanowsky A. J., Infante L., 2010, A&A, 513, A52
Seth A. C., et al., 2014, Nature, 513, 398
Spergel D. N. et al., 2003, ApJS, 148, 175
Strader J., et al., 2011, ApJS, 197, 33
Strader J., et al., 2013, ApJ, 775, L6
Thomas D., Maraston C., Bender R., 2003, MNRAS, 339, 897
Thomas P. A., Drinkwater M. J., Evstigneeva E., 2008, MNRAS, 389, 102
Tonry J. L., Blakeslee J. P., Ajhar E. A., Dressler A., 2000, ApJ, 530, 625
Turner M. L., Côté P., Ferrarese L., Jordán A., Blakeslee J. P., Mei S., Peng E. W., West M. J., 2012, ApJS, 203, 5
Urban O., Werner N., Simionescu A., Allen S. W., Böhringer H., 2011, MNRAS, 414, 2101
Voggel K., Hilker M., Richtler T., 2015, preprint (arXiv:1510.05010)
Weinmann S. M., Lisker T., Guo Q., Meyer H. T., Janz J., 2011, MNRAS, 416, 1197
Zentner A. R., Bullock J. S., 2003, ApJ, 598, 49
Zhang H.-X., et al., 2015, ApJ, 802, 30